TAMPEREEN TEKNILLINEN YLIOPISTO

JONI MAUNULA

COARSE PARTICLE PRE-SEPARATOR FOR HIGH TEMPERATURE SAMPLING

Master of Science Thesis

Tarkastaja: Professori Jorma Keskinen
Tarkastaja ja aihe hyväksytty 4.5.2011
Luonnotieteiden ja ympäristötekniikan
tiedekuntaneuvoston kokouksessa

TIIVISTELMÄ

TAMPEREEN TEKNILLINEN YLIOPISTO
Teknis-luonnontieteellinen koulutusohjelma
MAUNULA, JONI: Korkean lämpötilan esierotin
Diplomityö, 60 sivua
Toukokuu 2011
Pääaine: Teknillinen fysiikka
Tarkastaja: Professori Jorma Keskinen
Avainsanat: kloorikorroosio, alkalikloridi, savukaasu, virtuaali-impaktori

Halu vähentää hiilidioksidipäästöjä ja käyttää halvempia polttoaineita on kasvattanut tarvetta polttaa vaikeampia jäte- ja biomassapohjaisia polttoaineita. Nämä polttoaineet vaikuttavat kattilan toimintaan ja voivat aiheuttaa vakavia ongelmia. Poltossa muodostuvat pienhiukkaset ja kondensoituvat höyryt voivat reagoida kattilapintojen kanssa, etenkin lämmönsiirtopinnat ovat alttiita likaantumiselle ja korroosiolle. Näiden ongelmien takana on usein alkalimetalleja sisältävät yhdisteet, jotka muodostavat matalassa lämpötilassa sulavia kerrostumia tulistimille.

Polttoaineen kloorin, rikin ja alkalimetallien pitoisuudet vaikuttavat merkittävästi tulistimilta löytyvien kerrostumien klooripitoisuuteen. Kloorin aiheuttaman tulistinkorroosion yksityiskohtia ei vielä tunneta tarkasti mutta sen tiedetään aiheutuvan pääasiassa tulistimille kondensoituvan kaliumkloridihöyryn vaikutuksesta. Jotkin bio- ja jätepolttoaineet voivat sisältää myös merkittäviä määriä bromia ja raskasmetalleja, kuten sinkki ja lyijy. Myös näillä yhdisteillä voi olla samankaltaisia vaikutuksia kuin alkalimetalleilla. Savukaasun ja lentotuhkan koostumuksen parempi tunteminen auttaa ymmärtämään ja estämään kloorikorroosion mekanismeja.

Tämän diplomityön tarkoituksena on kehittää ja testata näytteenottoperiaatetta alkalikloridien mittaamiseksi. Tietoa korroosioriskistä voidaan käyttää polttoainesuhteiden optimointiin, lisäaineiden syöttöön ja materiaalilämpötilojen säätöön. Työssä testatulla näytteenottimella on tarkoitus mitata kloori, kalium ja natrium pitoisuuksia ja sen tulisi kyetä erottamaan yhdisteitä niiden fysikaalisten ominaisuuksien perusteella. Korkea lämpötila, kiintoaine sekä kaasun ja lentotuhkan monimutkainen koostumus tekevät leijukattilan tulipesästä mittaamisen haastavaksi. Näytteen jäähtyessä tapahtuvien fysikaalisten ja kemiallisten muutosten ymmärtäminen ja kontrolloiminen on tärkeää edustavan näytteen saamiseksi.

Sekundaaritulistimet ovat herkimpiä alkalikloridien aiheuttamalle korroosiolle sillä siellä kuuma noin 850°C kaasu kohtaa kylmiä lämmönsiirtopintoja. Alkalikloridihöyry pitoisuuksia halutaan mitata tulistinten läheisyydestä sillä niiden määrä muuttuu kokoajan kemiallisten reaktioden sekä kondensoitumisen ja nukleoitumisen kautta.

Merkittävin alkalikloridеja vähentävä reaktio on sulfatoituminen, jota tapahtuu pääasiassa kapealla lämpötila-alueella sekundaaritulistinten läheisyydessä. Loput alkalikloridеista jää matkan varrelle kerrostumiin tai poistuu lentotuhkan mukana, alkaleista jopa kymmeniä prosentteja voi jäädä kerrostumiin ja poistua kattilatuhkan mukana.

Diplomityön ensimmäisessä osassa käydään läpi työn taustoja, miksi, mistä ja miten alkalikloridеja halutaan mitata. Kattilassa ja näytteessä tapahtuvat muutokset ja kattilan olosuhteet vaikuttavat mertkittävästi näytteenottimen toimintaan. Teoriaosuudessa käydään läpi kattilan ja näytteenottimen kannalta merkittävimpiä fysikaalisia ilmiöitä. Pienhiukkasten muodostumista ja kerrostumien muodostumista tapahtuu sekä kattilassa että näytteenottimessa.

Näytteenottimen toimintaa ja soveltuvuutta haastaviin olosuhteisiin kokeiltiin sekä laboratorio- että todellisissa kattilaolosuhteissa. Laboratoriotesteillä selvitettiin virtausnopeuden ja sondin kärjen muotoilun vaikutusta virtuaali-impaktorin erotustehokkuuteen. Todellisissa olosuhteissa selvitettiin etenkin näytteenottimen herkkyyttä likaantumiselle ja soveltuvuutta osaksi jatkuvatoimista mittalaitetta.

ABSTRACT

TAMPERE UNIVERSITY OF TECHNOLOGY
Master's Degree Programme in Science and Engineering
MAUNULA, JONI: Coarse particle pre-separator for high temperature sampling
Master of Science Thesis, 60 pages
May 2011
Major: Engineering Physics
Examiner: Professor Jorma Keskinen
Keywords: High temperature corrosion, alkali chloride, flue gas, virtual impactor

The combustion of challenging fuels has become more important in recent years. This development with other recent interests has increased the importance of superheater high temperature corrosion. The aim of this thesis is to test and develop furnace alkali chloride sampling device including coarse particle pre-separator operating as virtual impactor. This sampling device can be used to take fine particles, vapours and gas containing samples from furnace.

In this thesis is presented the background of alkali chloride sampling and flue gas processes. The analysis method, difficult conditions and sample processes gives limitations for sampling. Fine particle formation, deposition mechanisms and particle classification are reviewed in theory part. The sampling device under development and sampling environment are described in this thesis. At the measurements part of the thesis the pre-separator measurements and full scale tests are presented.

The sampling device and virtual impactor were tested in laboratory conditions at Tampere University of technology aerosol physics laboratory. The main focus of laboratory tests was to measure the collection efficiency of virtual impactor with different flow velocities and different probe constructions. The availability and operation of sampling device in field conditions was tested at full scale fluidized bed boilers.

The pre-separator is able to cut the coarse particles from the sample flow. Though, the sampling line and some parts of the sampling device before the pre-separator can exposure to fouling. The flow velocity has the strongest influence on the cut point diameter especially with lower velocities. However, the flow velocity and the viscosity have only a small effect on the collection efficiency at field conditions. The vapour sampling is a very sensitive to losses? and the consumption of pressurized air causes expenses.

PREFACE

This Master of Science Thesis was managed by Metso Power and conducted in cooperation whit Metso Automation, UPM-Kymmene and Tampere University of technology, aerosol physics laboratory. The thesis was written between October 2010 and May 2011.

I would like to thank Metso Power Oy for giving me the opportunity to carry out this interesting project for the company and especially my instructor Juha Roppo and Mikko Anttila, Asko Rantee and Tarmo Toivonen for their support and help. I would like to thank Professor Jorma Keskinen for supervising this thesis and my instructors Marko Marjamäki and Topi Rönkkö for their guidance during this thesis and my studies. I would also thank my co-workers at Metso Power, TUT aerosol physics laboratory, UPM-Kymmene and Metso Automation.

Finally, I am grateful to my supportive family and friends for their understanding and patience during my studies and my work for this thesis.

Tampere, May 2011

Joni Maunula

CONTENT

TERMS AND DEFINITIONS

Aerosol	**Collection of solid or liquid particles suspended in a gas**
APS	**Aerodynamic particle counter**
BFB	**Bubbling fluidized bed**
CFB	**Circulating fluidized bed**
DLPI	**Dekati low pressure impactor**
DOS	**Dioctyl sebacate**
ELPI	**Electrical low pressure impactor**
Fouling	**Deposition formation in convectional parts of boiler**
FTIR	**Fourier transform infrared spectroscopy**
High temperature corrosion	**Chloride induced corrosion at high temperatures**
ISE	**Ion selective electrode**
Isokinetic sampling	**The flow velocity in sampling equals the flow**
RBDA	**Recovery boiler dust analyzer**
SMPS	**Scanning mobility particle sizer**
Superheater	**Converts saturated or wet steam to dry steam**
Supersaturation	**Vapour pressure larger than saturation pressure**
Vapour	**Gas phase substance at temperature lower than critical point**

SYMBOLS

λ	[m]	Free mean path
σ	[N/m]	Surface tension
η	[kg/(m s)]	Viscosity
ν	[m^3]	Molecular volume
ρ_p	[kg/m^3]	Particle density
ρ_g	[kg/m^3]	Gas density
C_c	[-]	Slip correction factor
D	[m]	Characteristic diameter
D_j	[m]	Jet diameter
d_p	[m]	Particle diameter
D_p	[m]	Particle diameter
d_{50}	[m]	Diameter with 50% collection efficiency
g	[m/s^2]	Gravitational acceleration
k	[J/K]	Boltzmann constant
K_R	[-]	Kelvin ratio
M	[kg/mol]	Molar mass
N	[-]	Number of particles
p	[Pa]	Pressure
p_d	[Pa]	Saturation pressure on particle surface
p_s	[Pa]	Saturation pressure
r_c	[m]	Critical radius
R	[J/(mol K)]	Molar gas constant
Re	[-]	Reynolds number
S	[-]	Saturation ratio
Stk	[-]	Stokes number
Stk_{50}	[-]	Stokes number for d_{50}
T	[K]	Temperature
∇T	[K/m]	Temperature gradient
U	[m/s]	Flow velocity
V_{ts}	[m/s]	Settling velocity

1. INTRODUCTION

Attempts to decrease greenhouse gas emissions have increased the importance of the utilization of biomasses and waste fuels in boilers for energy production. However, these fuels can influence the boiler operation and cause problems. Fine particles and condensable vapours released from the fuel interact with the heat exchange surfaces of the boiler. In power-producing boilers the main problems are usually superheater fouling and corrosion, because the great temperature difference between the heat exchanger surface and the flue gas. These problems are usually related to alkali metal-containing particles and vapours that can condense on surfaces and are responsible for the creation of low-melting point sticky deposit on the heat exchanger surfaces (Sippula 2010).

Alkali metals act as a conduit for chlorine and transport it to the heat exchange surfaces. The destructive effect of alkali metals and chlorine is associated with bio and waste fuels that usually contain only small amounts of sulfur. Currently the high corrosion rate is assumed to be caused by gaseous KCl that condenses or sublimates on the heat transfer surface. Some bio and waste fuels may also contain high levels of heavy metals, like Zn and Pb, which have a similar effect on the ash behavior as the alkali metals (Enestam et al. 2003, Blomberg 2006).

The determination of the flue gas composition in full scale furnaces is important for understanding and preventing the high temperature corrosion. When measuring in the furnace area, the main challenges are the high temperatures, the high concentrations of particles in the flue gas and the complexity of the gas composition. In fouling and corrosion studies fly-ash particle measurements have played an important role. In order to collect representative sample for analysis it is important to control the sample cooling and chemical and physical evolution (Vainio et al. 2009, Skrifvars et al. 2004).

The aim of this thesis is to develop and test sampling device to measure concentrations of alkali chlorides from the power boiler furnace. The information of corrosion risk can be used to control furnace atmosphere and material temperatures. The analyzer under development can measure chloride, potassium and sodium concentrations. The sampling device should be able to separate the flue gas species and the fine particle fractions by their physical properties. Understanding and controlling the flue gas transformation during sampling is important to collect representative sample.

This thesis consists of literature preview and measurements. The theoretical background of virtual impactor, possible losses and sample processes are presented in literature preview. The measurements are accomplished in laboratory conditions at Tampere University of technology and in field conditions in two full scale power boilers. The operation and collection efficiency measurements of virtual impactor are completed in TUT aerosol physics laboratory. At full scale, the availability on long time on-line sampling of sampling system is estimated.

2. BACKGROUND

2.1. Fluidized bed boiler

In fluidized bed boilers the combustion takes place in a bed of inert particles fluidized by primary air. This technology has been used since 1970s. The main success factors of the fluidized bed combustion technology have been the capability of handling a wide variety of solid fuels with low emissions. The properties of the difficult fuels and the behavior of fuel ash may limit the use of such fuels due to the increased risk of bed agglomeration, fouling and corrosion (Salmenoja 2000, Silvennoinen 2004).

2.1.1. Bubbling fluidized bed boiler

The bubbling fluidized bed (BFB) was the first version of the Fluidized bed technology and past decades has confirmed that it can be well suited to the use of difficult fuels such as high-moisture, high-ash and low volatile fuels. BFB combustor also allows over 100 mm fuel particles and fuels with lower caloric value. Despite the growing competition from the circulating fluidized bed in recent years, BFB has maintained an importance especially in smaller industrial applications and combustion of waste. Future technology development of BFB is likely to be improving fuel flexibility to increase the use of biomass and waste (Koornneef et al. 2007).

The fluidized bed is a 40–70 cm high layer of sand or other inert material that is being fluidized by primary air. In the BFB combustion, the NOx emissions are low due to the air staging and the CO emissions can be kept at a low level by controlling the combustion in the furnace. In BFB boiler practically all ash-forming matter in the fuel turns to fly ash and leaves the furnace with the flue gas. However, fuels also contain coarser impurities that drop to the bottom of the bed. Dense particles over 2 mm in size do not fluidize and they must be removed from the furnace (Hulkkonen et al. 2003, Silvennoinen 2004).

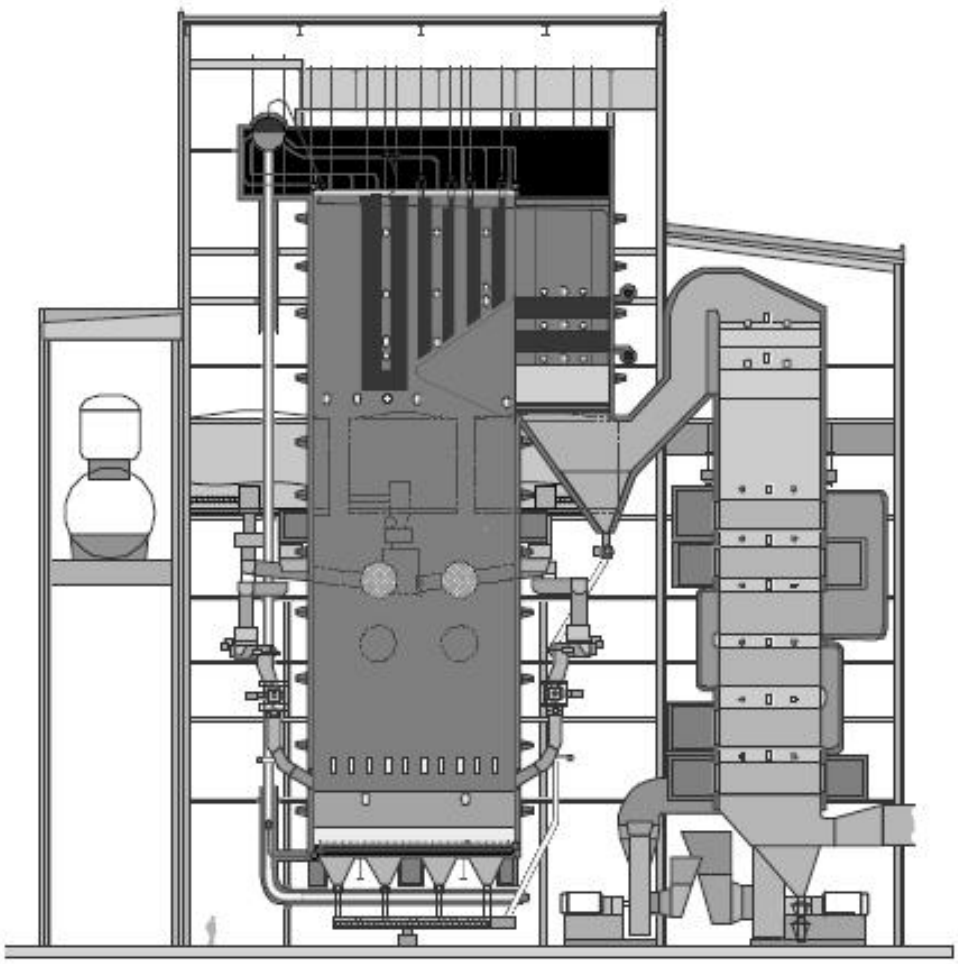

Figure 2-1: *Bubbling fluidized bed boiler, Metso HYBEX boiler*

In Metso HYBEX boiler (figure 2-1) the volatilized gases and fine fuel particles are combusted above the bed by secondary air after the hot sand has dried and volatized the fuel. The residual char and larger fuel particles are combusted inside the sand bed. The superheaters are located in upper part of the furnace and in the second pass. These boilers achieve a combustion efficiency of over 99% and the boiler efficiency can be over 90% depending on the fuel properties. The thermal capacity of HYBEX boilers varies from 10 to 300 MW_{th} (Metso 2010a).

2.1.2. Circulating fluidized bed boiler

The basic difference between BFB and circulating fluidized bed (CFB) is the fluidization velocity compared to the terminal velocity, which is higher for CFB. In CFB boilers the average size of bed material is also smaller. Additionally the sulphur removal is more efficient in circulating fluidized bed boilers. In the CFB boilers higher

steam parameters are also possible. In CFB, the solid material is entrained in the air flow more equally along the combustor height, mixing is better and the temperature more equal (Koornneef et al. 2007)

In CFB combustion fuel and limestone are injected into the furnace or combustor. The particles are suspended in a stream of upwardly flowing primary air, 50–60% of the total air. While combustion takes place at 840–900°C, particles under 450 μm are ejected out of the furnace with flue gas velocity of 4–6 m/s. Coarse particles are then collected by cyclone and circulated back into the furnace, the cut point of these industrial cyclones are usually about 50 μm. The sections of superheaters can be located after the cyclone, in the furnace and in the loop seal (Kavidass et al. 2000, Rönkkömäki 2008).

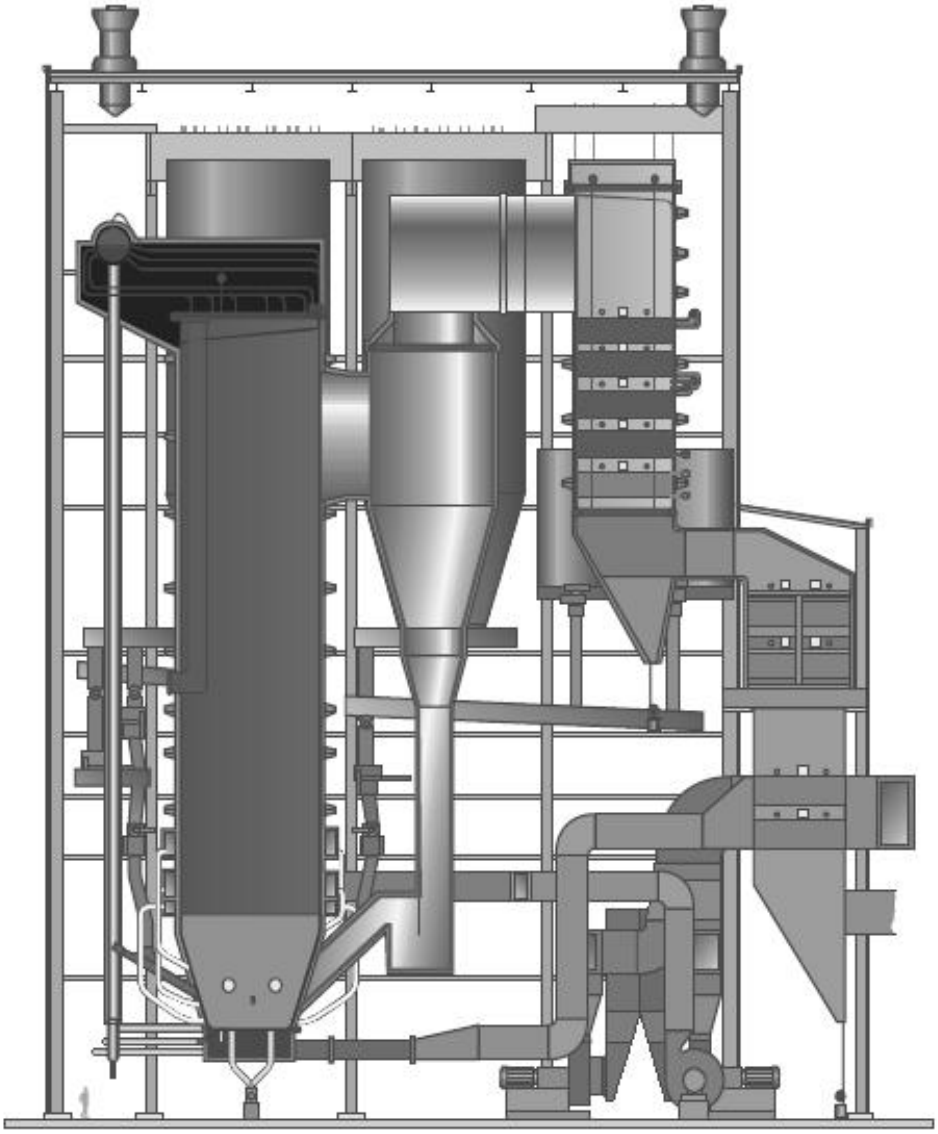

Figure 2-2: *Circulating fluidized bed boiler, Metso CYMIC boiler*

The foremost advantage of Metso CYMIC boilers (figure 2-2) is the high fuel flexibility, from 100% coal to 100% biomass and any combination in between. The CFB process provides excellent emission control achieved through a constant and relatively low combustion temperature. Excellent mixing and long solids retention time of solids advance efficient burning. The CYMIC boiler cyclone design is based on standard cyclone and loop seal components which enable smaller heat losses. The thermal capacity of these boilers varies from 50 to 600 MW_{th} (Metso 2010b).

2.2. High temperature superheater corrosion

The material loss in superheaters is one of the biggest threats in commercial boilers resulting in an increase in the operating costs and being a common reason for boiler shutdown. The factors that cause high temperature corrosion are not fully understood but it is known to be strongly related to the potassium chloride vapour concentration. Metal loss can also occur due to oxidation, sulphidation and erosion-corrosion. Chlorine-induced corrosion (figure 2-3) is a common in waste and biomass combustions where corrosion can cause very rapid metal loss. Corrosion rate can increase dramatically if molten deposits are formed (Makkonen 1999).

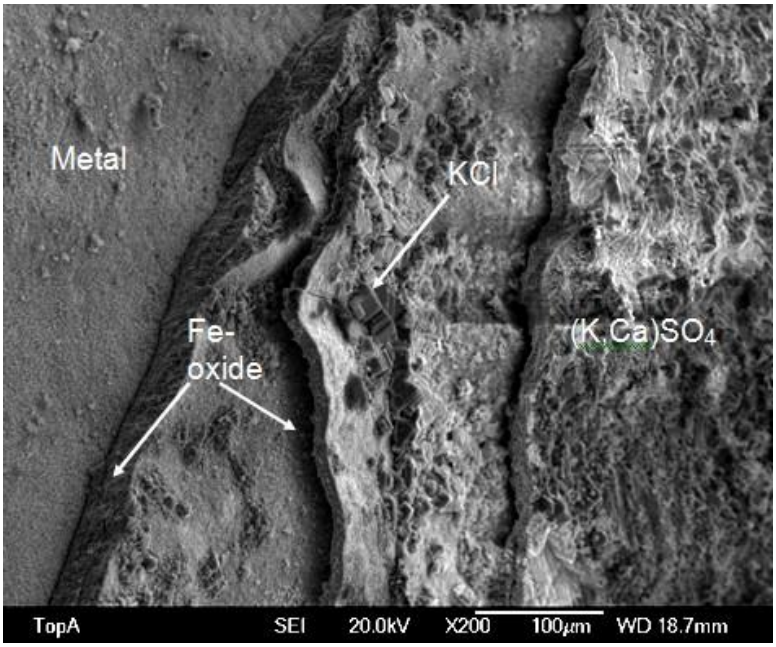

2-3: *High temperature superheater corrosion*

High temperature corrosion of superheaters is strongly connected to ash-deposition on the tubes. The mechanisms of fouling on boiler surfaces include condensation of vapours, inertial impaction of coarse particles, thermophoresis and diffusion of fine particles with chemical reactions. The order in which these phenomena occur, and the relative rates, affect to the morphology and mechanical properties of the deposits. The

deposit formation also depends on the boiler design and operation. During the combustion of biomass, large amounts of Cl and S together with volatile alkali metals, mainly potassium, are released as vapours to the flue gas (Riedl et al. 1999, Baxter et al. 1998).

In general the superheater high temperature corrosion (figure 2-4) during combustion of fuels containing biomass is depended on chlorine and alkali metals, especially potassium chloride vapours. Alkali chloride induced superheater corrosion is possible at material temperatures higher than 450°C, depending on tube materials. Chlorine deposition in the form of alkali chlorides, especially in the form of the potassium chloride, dominates strongly over the deposition of chloride in other compounds (Aho et al. 2007).

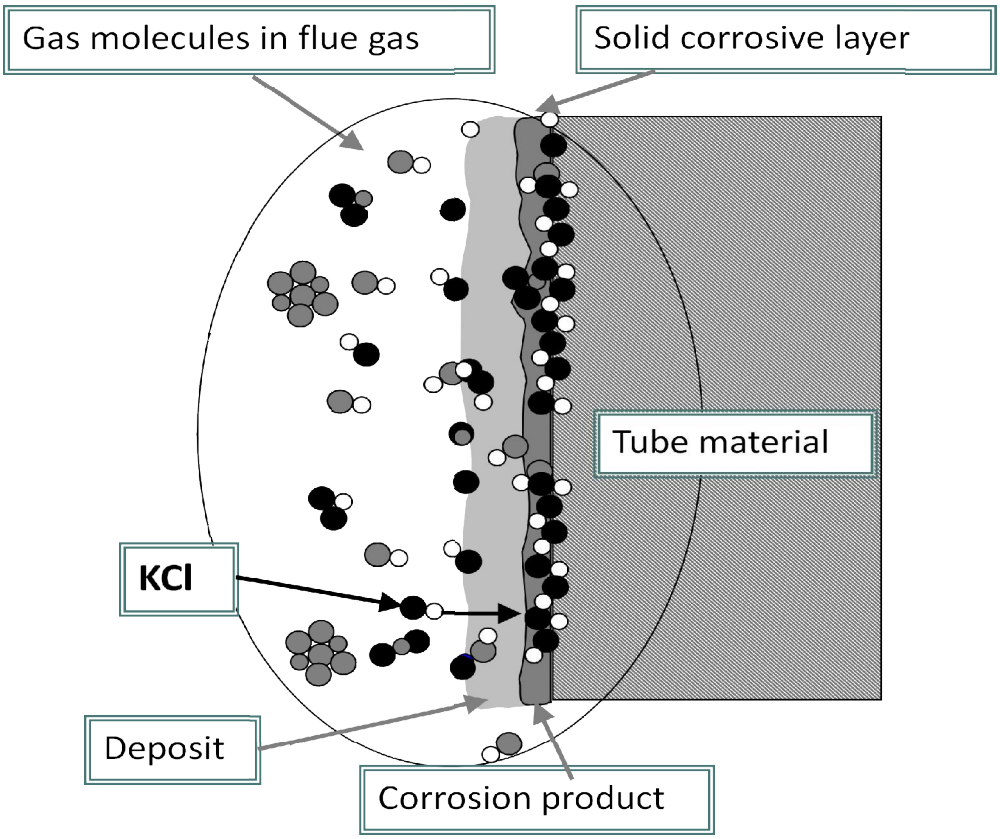

Figure 2-4: *Alkali chloride induced corrosion*

Attempts have been made to prevent the chloride deposition by mixing sulphur-rich fuels, for example peat, with corrosive fuels. Co-combustion of peat transfers the alkali from the vapours and fine particles to the coarser ones by sorption and/or reaction with the increased amount of residual ash particles. Potassium can also be captured by additives containing compounds like sulphur or aluminum silicate. However, more effective way to apply sulphation is to add chemicals directly forming SO3 (Aho et al. 2007, Kassman et al. 2011).

2.3. Flue gas of fluidized bed combustion

The fly ash mass size distribution from large-scale combustion of biomass consists of two modes that have different chemical compositions due to different mechanism of formation. The fine mode particles in the submicron size range (< 1 μm) are formed mainly from vaporized constituents (K, Na, S, Cl and heavy metals). These aerosols are dominated by potassium compounds (K_2SO_4, KCl and K_2CO_3) in biomass combustion, while aerosols from waste combustion contain also relevant amounts of sodium and heavy metals. The supermicron particles (> 1 μm) are formed mainly from ash particles entrained from the fuel bed, and they consequently have a higher concentration of refractory ash components such as Ca, P, Si, Al and Mn (Strand et al. 2004, Jöller et al. 2007).

2.3.1. Release of vapours

Several factors are known to influence the release fractions of ash forming species. As can be expected, the combustion temperature affects which species can volatile, also the oxidizing/reducing conditions affects the release of ash. The fuel particle size and structure influence to the burning condition and vaporization. The fuel composition affects the release via complex, and not well understood, chemical and physical mechanism. For example the presence of chloride affects the formation of alkali vapours (Strand et al. 2004, Sippula 2010).

Equilibrium calculations have shown that in high temperatures before boiler inlet (> 900 °C), potassium primarily exists as KCl(g) and as KOH(g), while sulphur and excess chlorine are present as SO_2(g) and HCl(g) respectively. With temperatures relevant to biomass and waste combustion, lead and other heavy metal oxides can be the first significant vapour-phase compounds forming condensed species in the flue gas (figure 6). In chlorine-rich systems significant fractions of heavy metal chlorides ($ZnCl_2$, $PbCl_2$) may be formed. These compounds can also cause corrosion (Riedl et al. 1999, Sippula 2010).

The chlorine concentration has a considerable role in the behavior of alkali metals. Chlorine contributes to the volatilization of alkali metals, thus increasing the amount of alkali compounds in the gas phase, and formed alkali chlorides are quite stable and gas-to-particle conversion occurs by homogeneous nucleation or condensation rather than by chemical reaction. When burning fuels with low chlorine concentrations the chlorine is the limiting factor for formation of KCl and alkali metals form initially alkali hydroxides which later form sulphates and carbonates (Jokiniemi et al. 2009, Miettinen Westberg et al. 2003).

2.3.2. Aerosol particle formation

The behavior of ash-forming species is significantly influenced by the chemical and physical properties of released species, combustion environment and cooling conditions. The saturation of fine particle forming species can raise true chemical reactions and flue gas cooling leading to gas-to-particle conversion at high temperatures. The rate of nucleation and condensation reactions determines the chemical composition of the particles as well as the deposits and relative amounts of the gas pollutants HCl and SO_2 (Strand et al. 2004, Christensen et al. 2000).

Aerosol formation during the combustion process takes place because some volatile compounds are released from the fuel bed to the gas phase. The main gas-to-particle species in fluidized bed boiler flue gas are alkali sulphates and chlorides, potassium carbonate and heavy metal oxides and chlorides. During biomass combustion the main constituents of the submicron particle fraction are usually potassium sulfate and chloride. A theoretical analysis has shown that gas-to-particle conversion occurs by homogeneous nucleation of K_2SO_4 and heavy metal oxide (ZnO and PbO) particles, which act as condensation nuclei for KCl (Strand et al. 2004, Jöller et al. 2007).

2.3.3. Potassium

When flue gas cools the first processes affecting potassium containing substances are KOH(g) conversion to KCl(g) and there sulphation to potassium sulphate (figure 2-5). According to chemical equilibrium all sulphur should be bound as solid K_2SO_4 at temperatures below 900 °C. However, the reactions (presented below) are very slow at temperatures below 800 °C and the sulphation is limited to a temperature interval 800–900°C. Sulphation of solid potassium chloride is very slow compared to the gas phase sulphation reaction. The main sulphur containing species in biomass combustion at temperatures below 800 °C are K_2SO_4(s), SO_2(g) and smaller amounts of Na_2SO_4(s) (Riedl et al. 1999, Zeuthen et al. 2007).

$$KOH(g) + HCl(g) \longrightarrow KCl(g) + H_2O(g)$$

$$2SO_2(g) + O_2(g) \rightleftarrows 2SO_3(g)$$

$$2KCl(g) + H_2O(g) + SO_3(g) \rightleftarrows K_2SO_4(c) + 2HCl(g)$$

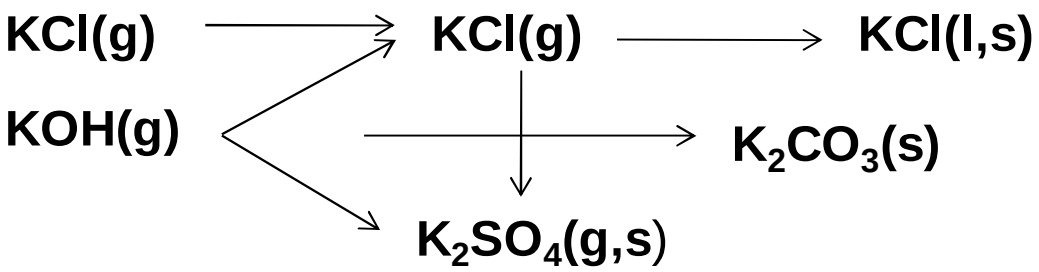

Figure 2-5: *Possible pathways to particles for evaporated potassium species.*

Since the sulphation reaction together with the cooling itself causes the supersaturation of K_2SO_4 the homogeneous nucleation is possible at temperatures around 860–760 °C. While cooling proceeds to the temperature of 650 °C these formed nanometer-sized particles can act as condensation nuclei for the subsequent condensation of chloride vapours. When temperature decreases to less than 500 °C all potassium should be in particle phase (figure 2-6). Currently the question whether alkali metal condensation occurs on seed particles or with homogeneous nucleation is not answered (Christensen et al. 1998, Livbjerg 2001, Sippula 2010).

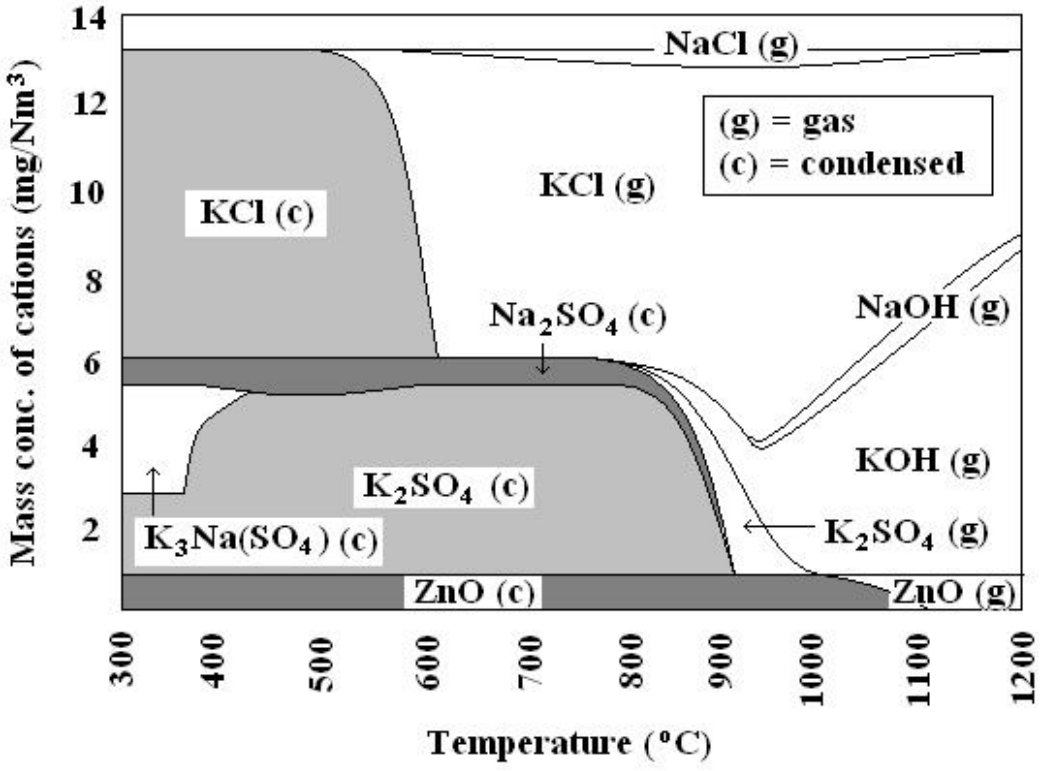

Figure 2-6: *A typical equilibrium calculation result with wood fuel (Sippula 2010).*

2.3.4. Supermicron particles

The supermicron particles are formed from ash particles, bed material and additives entrained from the fuel bed. These particles contain high amounts of calcium, silicon and other nonvolatile compounds. The amount of supermicron particles entrained from the bed increases with the boiler load because of the higher flue gas velocities. The amount is strongly dependent on the combustion technology. The average particle size of the count distribution of fly ash fraction is usually larger than 5 μm. The biggest particles in the flue gas channel might be few hundred micro meters in size (Brunner et al. 1998).

Abd-Elhady et al [2004] has noted in laboratory tests that most of the particles in the first fouling layer deposited on the heat exchangers tube have diameter less than 40 μm and the average diameter of those particles is about 15 μm. The coarse over 10 μm fly ash particles are mainly found on the windward side of the probe transported by the inertial impaction. The deposition on the leeward side of the probe is formed by turbulence and higher concentration of fine particles are found there. Fine particles are also collected by diffusion and thermophoresis (Peltola et al. 1999).

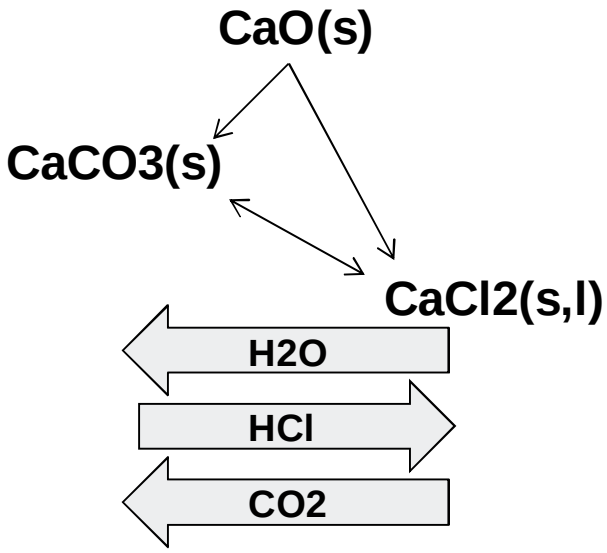

Figure 2-7: *Calcium pathways in the flue gas*

There are indications that the calcium-rich mineral grains consist of calcium oxalate (CaC_2O_4) and are released from the fuel as mineral particles roughly 2–10 μm. These calcium oxalates form CaO particles at higher temperatures (> 800 °C) and CaCO3 at lower temperatures (< 800 °C). Figure 2-7 illustrates the reactions and effect of other flue gas compounds for calcium compounds. The calculations imply that, depending on the operating conditions, some HCl may be absorbed by CaO at relatively high temperatures (Skrifvars et al. 2004, Partanen 2004).

2.4. Alkali chloride analyzer

2.4.1. RBDA

The analyzing method used with developed sampling device is based on the Recovery Boiler Dust analyzer (RBDA) technology presented in figure 2-8. The RBDA operates by dissolving the flue-gas fly ash sample in ion- exchanged water and analyzing the ion concentration of the sample solution potentiometrically by means of Ion-Selective Electrodes (ISEs). ISEs, which in this case are able to measure chloride, potassium and sodium ions on-line, are sensors that convert the activity of a specific ion dissolved in a solution into an electrical potential (Dekati 2002).

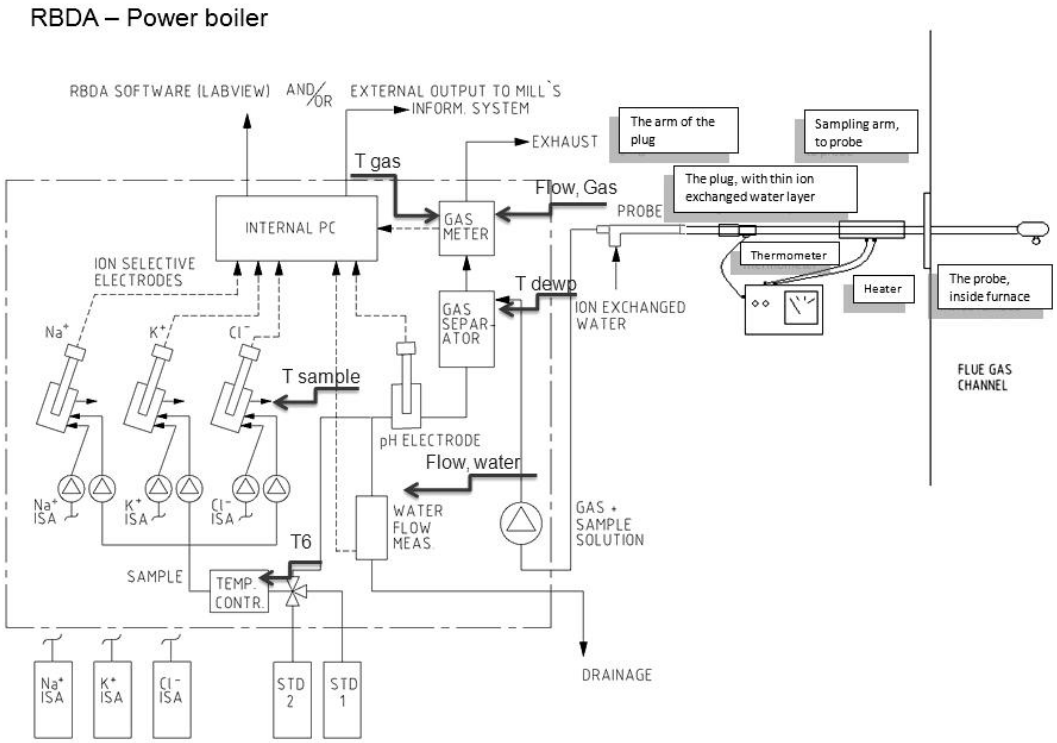

Figure 2-8: *Flow chart of the RBDA with inboard measurement points*

In a recovery boiler, the sample consists mainly of particles less than 1µm in size, while in a fluidized bed boiler; the sample contains much wider size distribution of particles. Flue gas contains also other disturbing compounds, mainly hydrogen chloride and alkali sulphates. In the used method the total chloride and gas phase chloride (HCl) are measured. The amount of alkali chlorides (condensed chloride) can be calculated by subtracting the gas phase Cl from total Cl. The sampling probe should be able to separate gas phase and condensed chloride on-line from furnace.

(2-1)

2.4.2. Power boiler analyzer

In a power boiler application the sample is analyzed after a short concentrating period in a bubbling container. Concentrating sampling allows to measure greater concentrations from the container and to use same analyzer for both the gas and total samples. The concentrating time is about 10 minutes which is enough for corrosion monitoring of the boiler. The concentrating sampling makes possible to take and analyze several samples with one analyzer. Measured species hydrogen chloride and alkali chlorides are very soluble to water and only a few percent of these compounds can passes through the bubbling container.

2.5. High temperature sampling

There are certain properties that must be considered when sampling aerosols at high temperatures, since a number of dynamic physical and chemical processes are in progress in the aerosol system. The use of sampling and cooling devices can affect the dynamics of processes while sampling, especially when sample contains alkali or heavy metal vapours. In this case, the most interesting processes are the formation of alkali sulphates and nucleation/condensation of alkali chlorides, also reactions of hydrogen chloride must be considered. These and other processes will change the original size distribution and particle and gas composition during sampling (Strand et al. 2004).

Dynamic flue gas processes, especially condensation of saturated vapours, can raise the risk of losses when sampling these species. Thermophoresis must also be considered if cold surfaces are present. Condensation and thermophoresis with other particle deposition mechanisms can expose the sampling or cooling devices for fouling especially when sampling from fluidized bed boilers where high suspension atmosphere and vapours are present. Fouling can disturb sampling device operation, cause shutdown and in worst case break the device.

A high temperature also limits available materials and devices. Most of the analyzers and sample handling devices operate only at room temperature or near it. This affects the possible measurement set ups. High temperatures and fouling conditions can additionally limit the live time of the sampling devices. Because of the heat expansion the construction of sampling probe and devices must be very simple and the expansion must be considered when designing sampling device for high temperatures.

3. AEROSOL PROCESSES

3.1. Fine particle formation

The formation and growth of aerosol particles by condensation is the most important mass-transfer process between the gas phase and the particulate phase in flue gas. These processes commonly require a supersaturated vapour or condensation nuclei. The supersaturation can be produced by chemical reactions and/or cooling. The reverse of the growth by condensation is evaporation that is involved in the production of nuclei. Condensation-evaporation process is an equilibrium process and it is strongly related to the saturation ratio S, the ratio of the partial pressure to the saturation pressure. When the saturation ratio is greater than one, the gas-vapour mixture is supersaturated (Hinds 1999).

3.1.1. Nucleation

The process where gaseous vapour molecules combine to form clusters large enough to remain stable is called homogeneous nucleation. The smallest radius of stable clusters is called critical radius (r_c) and a smaller cluster can either grow or evaporate. The critical radius is strongly depended at surface tension (σ), temperature (T) and saturation ratio (S). The other symbols in the equation are molecular volume (v) and Boltzmann constant k.

$$r_c = \frac{2\sigma v}{kT * lnS} \tag{3-1}$$

The rate of homogeneous nucleation is very sensitive to the saturation ratio and surface tension of the nucleating species (Baxter 2008, Christensen et al. 1996).

Once nucleation clusters are available in the condensed phase the effect progresses very rapidly given the increased available surface area. Increased area increases the rate of nuclei growth because molecular kinetic energy is more easily dissipated on a large surface. Nucleation is rare process in nature because it usually requires supersaturation and usually there is presented surfaces where condensation can occur before nucleation is possible. In flue gas supersaturation and nucleation can be possible due cooling and chemical reactions (Baxter 2008).

3.1.2. Particle growth

Condensation occurs more readily than nucleation because the formation of stable clusters usually requires supersaturation. Condensation occurs due to a pressure gradient between the partial pressure of a species in the gas and the pressure of the species at the surface of a particle. Particle growth rate is therefore limited by the diffusion of particles through the gas for particles larger than the mean free path. For particles smaller than the mean free path, growth is limited by the surface area of the particle (Baxter 2008, Hinds 1999).

The curvature of the surface modifies the attractive forces and decreases the effect of partial pressure for small particles; this effect is called the Kelvin ratio K_R. The K_R is defined by the rate of saturation pressure on the surface (p_d) and saturation pressure far from the surface (p_s). The M in the equation is molar mass, R the molar constant, ρ the density and d_p the particle diameter (Baxter 2008, Hinds 1999).

$$K_R = \frac{p_d}{p_s} = exp\left(\frac{4\sigma M}{\rho R T d_p}\right) \tag{3-2}$$

After nucleation and condensation particles can grow further by coagulation. Coagulation of aerosol is a process where aerosol particles collide with one another, due to a relative motion between them and adhere to form larger particles. Because the rate of coagulation is proportional to N^2, it is rapid at high concentrations but slows as coagulation proceeds. In the case of solid particles, the process is called agglomeration, and the resulting particles are known as agglomerates. Particle size, chemical composition and process conditions determine the properties of agglomerates (Hinds 1999, Jokiniemi et al. 2009).

3.2. Deposition mechanisms

In combustion devices the main mechanisms which cause particle deposition are gravitational settling, inertial impaction, thermophoresis and particle diffusion. Gravitational settling and inertial impaction are the main deposition mechanism for large particles while thermophoresis and particle diffusion are more important with fine particles. In addition to particle formation and deposition processes, during combustion and flue gas cooling direct condensation of aerosol forming species on furnace and boiler walls occurs (Jöller et al. 2007).

3.2.1. Coarse particles

The gravitational field exerts a force pulling the particle down. As the particle begins to move, the gas surrounding the particle exerts an opposing drag force. After a short period of acceleration the drag force equals the gravitational force and the particle reaches its terminal settling velocity V_{ts} (equation 3-3). At higher Reynolds numbers (Re), the observed settling velocity is lower than predicted by the next equation where C_c is the slip correction factor and η is the viscosity. For spherical particles the gravitational settling velocity can be expressed as in equation 3-4, where the C_d is the drag coefficient (Baron et al. 2005)

$$V_{ts} = \frac{\rho_p d^2 g C_c}{18\eta}, Re_p < 0.1 \tag{3-3}$$

$$V_{ts} = \left(\frac{4\rho_p C_c d_p g}{3\rho_g C_d}\right) \tag{3-4}$$

Impaction is a special case of curvilinear motion where particles whose inertia exceeds a certain value are unable to follow the streamlines. The importance of this inertial impaction mechanism increases with increasing particle size (d_p) and increasing flow velocity (U). The inertial impaction can be studied by the use of the dimensionless Stokes number (Stk), which is the ratio of the particle stopping distance to the characteristic dimension (D) of the obstacle. Impaction finds many applications in the collection, separation and measurement of aerosol particles (Hinds 1999, Baron et al. 2005).

$$Stk = \frac{\rho_p d_p^2 C_c U}{18\eta D} \tag{3-5}$$

3.2.2. Fine particles

When a temperature gradient (∇T) is established in a gas an aerosol particle experiences a force in the direction of decreasing temperature. The movement of the particle that results from this force is called thermophoresis. When a cold surface is proximate to a warm gas, thermophoresis causes particles in the gas to be deposited onto the surface. For particles smaller than the free mean path ($d < \lambda$) the force and the velocity (V_{th}) of thermophoresis are results of a greater transfer of momentum from the gas molecules on the hot side of the particles and are independent of particle size (Hind 1999).

$$V_{th} = -\frac{0{,}55\eta\nabla T}{\rho_g T}, for\ d < \lambda$$

(3-6)

Brownian motion is the irregular motion of a particle in still air caused by random variations in the relentless bombardment of gas molecules against the particle. Diffusion of particles J (equation 3-7) is the net transport of these particles in a concentration gradient ($\frac{\partial N}{\partial x}$) and it's always from higher concentration to lower concentration. Because of this, diffusion always generates a net transport of particles to the walls where they deposit. Diffusion is the primary transport and deposition mechanism of particles less than 0.1 μm in diameter (Hinds 1999, von der Weiden et al. 2009).

$$J = -D\nabla N$$

(3-7)

$$D = \frac{kTC_c}{3\pi\eta d_p}$$

(3-8)

When a superheater wall exposed to a vapour is cooled below the saturation temperature, condensation will occur on the surface. Film condensation is a mode where condensate covers the wall by very thin film. The film thickness will grow as more condensate is diffused on the wall. Condensate flow rate depends on the temperature difference. If the condensate does not wet the wall, because either it is dirty or it has been treated with a nonwetting agent, the mode is called dropwise condensation. Droplets of condensate nucleate at small pits on the surface and grow rapidly by direct vapour condensation (Mills 1999).

3.3. Particle classification

3.3.1. Filtration

Filtration is one of the most widely used techniques for aerosol measurement and particle separation. When aerosol passes through a filter particles deviate from the streamlines due to several mechanisms. As a result, particles may collide with the filter surface and become deposited on it. Particle penetration is dependent on several parameters including the particle size, filtration velocity and filter thickness, fiber diameter and fiber packing density. The three primary collection mechanisms are illustrated in figure 3-1 (Baron et al. 2005, Richardson et al. 2006).

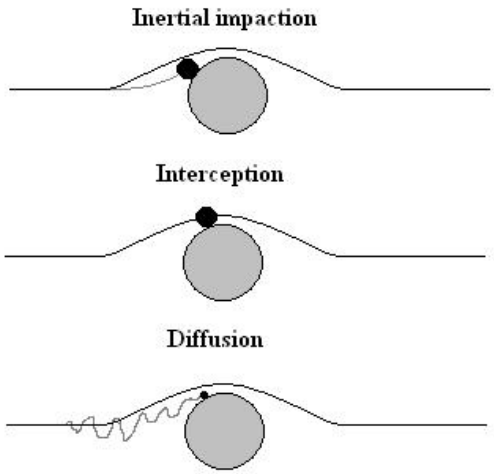

Figure 3-1: *Filter particle caption mechanisms (Richardson et al 2006)*

Diffusion, interception and impaction are effective over different particle sizes (figure 3-2). Small particles generally do not follow the streamlines but continuously diffuse away from them. Particles with a finite mass and moving with the flow may not follow the streamlines exactly due to their inertia. This collision is called inertial impaction and it depends on the particle size and the flow velocity. Even if the trajectory of a particle does not depart from the streamline, a particle may still be collected (interception) if the streamline brings the particle center to within one particle radius from the fiber surface. Once the particle is collected on a surface, it would adhere to it due to the van der Waals force (Baron et al. 2005, Richardson et al. 2006).

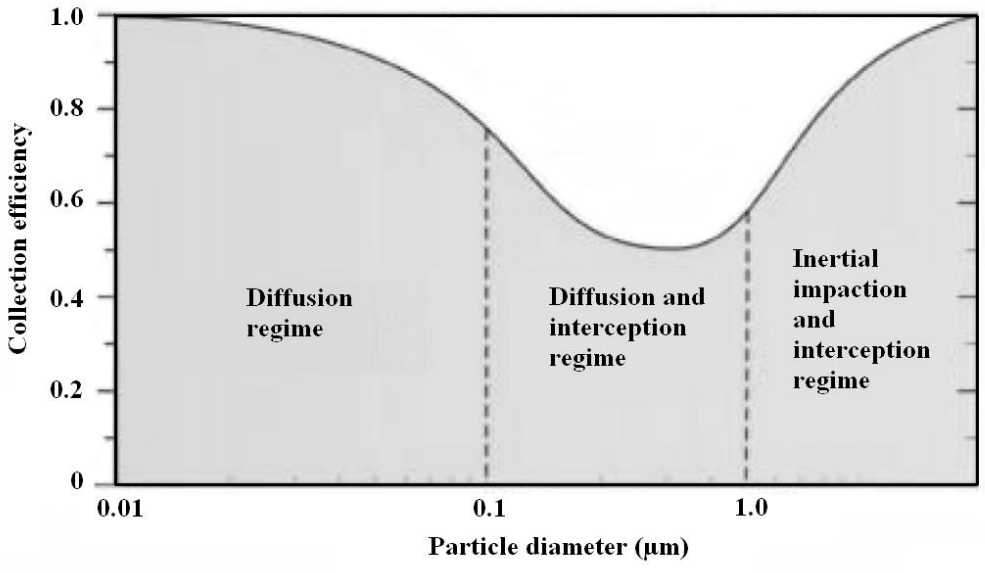

Figure 3-2: *Filter efficiency versus particle size (Richardson et al 2006)*

3.3.2. Impactors

All inertial impactors operate on the same principle. As shown below an aerosol is passed through a nozzle and the output stream directed against a flat plate. The impaction plate deflects the flow to form an abrupt 90° bend in the streamlines and collide on the flat plate. Smaller particles can follow the streamlines and avoid hitting the impaction plate. Thus, an impactor separates aerosol particles into two size ranges; particles larger than a certain aerodynamic size are removed from the airstream and those smaller than that size remain airborne and pass through the impactor (Hinds 1999).

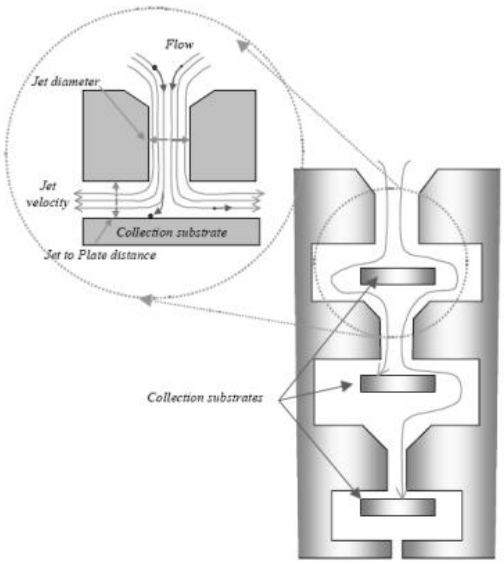

Figure 3-3: *Cross-sectional view of a cascade impactor*

In virtual impactor the impaction plate is replaced by a collection probe as shown in figure 3-4. Particles with inertia sufficient to cause them to impact on an impaction plate of a convectional impactor are thrown into the collection probe. Smaller particles can follow the streamlines radially away from the jet axis by the major flow. The cutoff diameter (d_{50}) of impactor or virtual impactor can be calculated by equation 3-9, where D_j is the jet diameter. For conventional impactor with circular jet the Stk_{50} is 0.24, for virtual impactor Stokes number depends on ratio of minor and major flows (Hinds 1999).

(3-9)

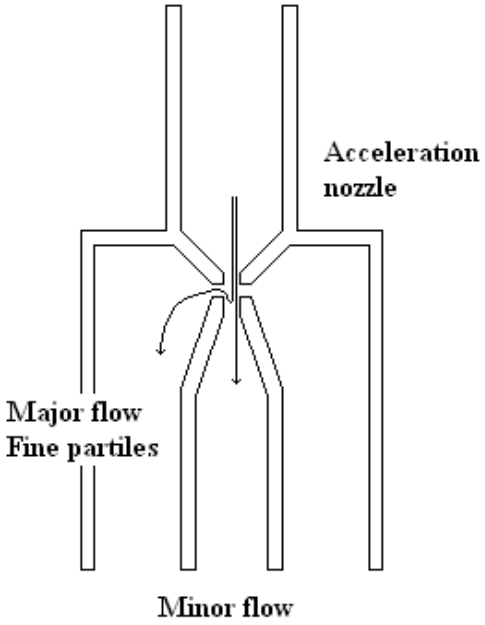

Figure 3-4: *The principle of a virtual impactor*

4. SAMPLING DEVICE

The sampling device (figure 4-1) consists of the probe inside the boiler and the circulating part outside the boiler wall. The sampling probe containing the pre-separator and the filter is located inside the circulating part of the sampling device. The flow is made by an ejector and it is controlled by the venturi. The operation of the venturi is based on the reduction of the fluid pressure in a constricted section of pipe. The temperature inside the boiler is around 850°C and the sample has been cooled to less than 500°C before the filter.

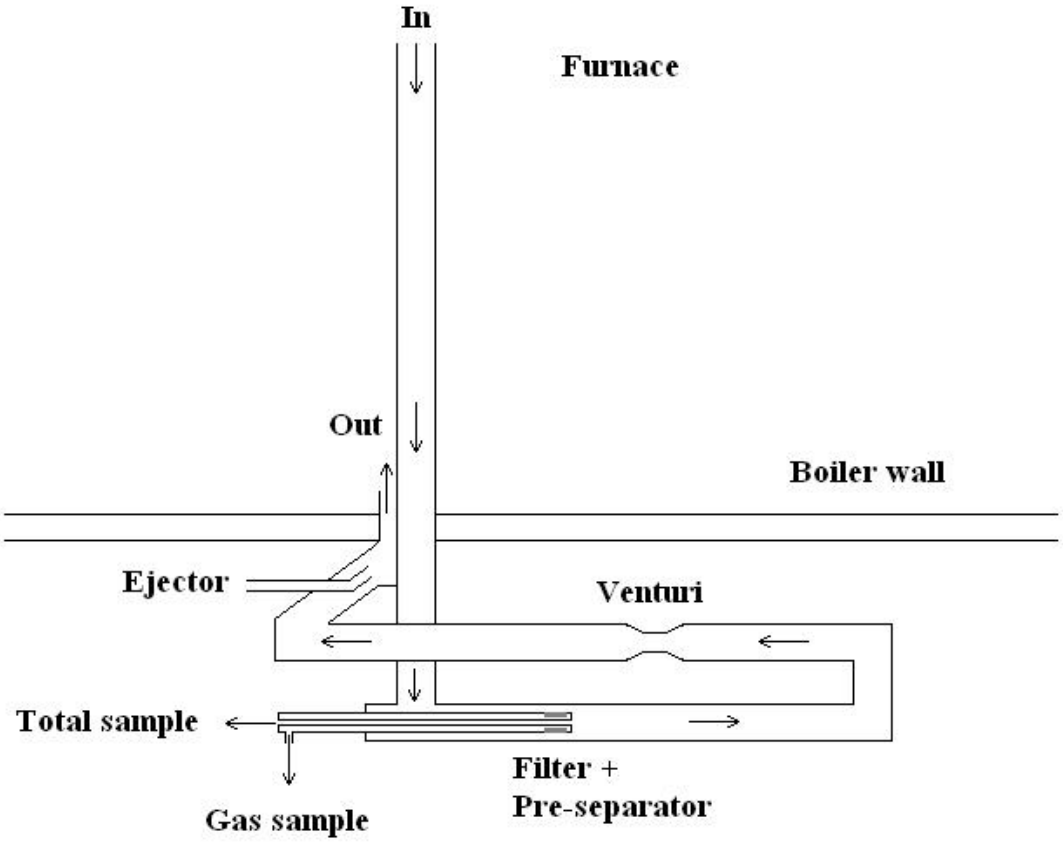

4-1: *Measurement setup for the full scale boiler*

4.1. Sampling environment

The sampling location in the furnace is close to secondary and tertiary superheaters at temperature about 850 °C in normal boiler condition. In the sample intake area the flue gas contains a lot of coarse particles which have escaped from the fuel and bed and condensable vapours. The location is selected because secondary and tertiary superheaters are the most sensitive to the high temperature corrosion. In the flue gas at high temperatures, chlorides are mainly in HCl and alkali chlorides while volatilized potassium and sodium are mainly in chlorides and sulphates.

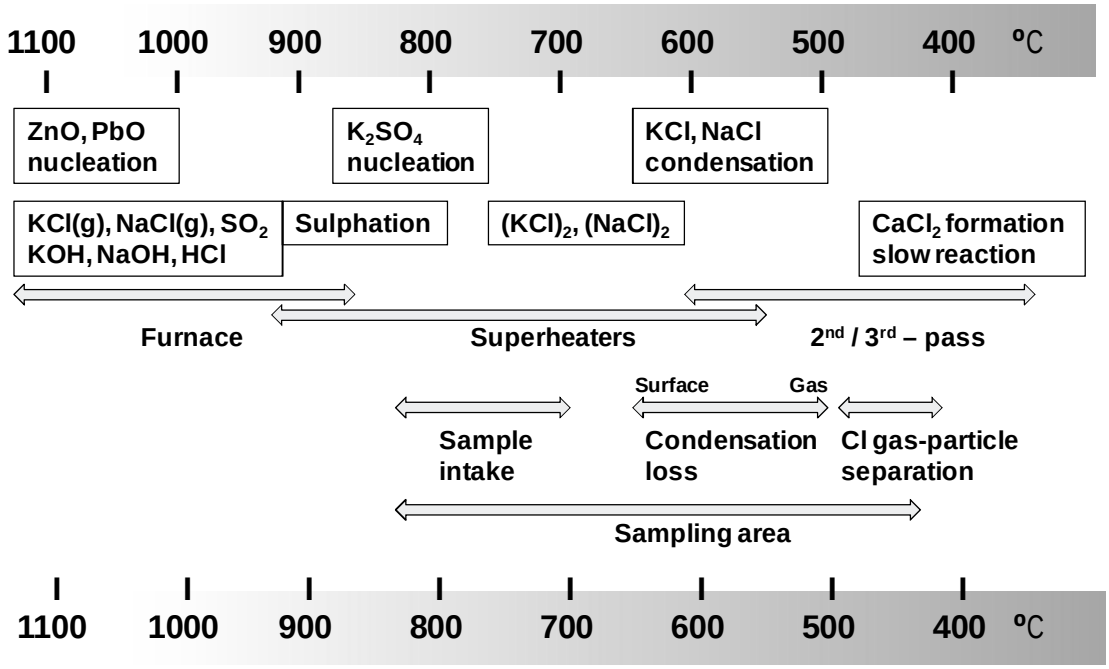

Figure 4-2: *Physical and chemical changes in the fluidized bed boiler flue gas.*

Figure 4-2 presents the temperature areas of physical and chemical changes with sampling area. The boiler temperature range presented is at typical boiler condition and with partial boiler load the temperatures can be lower in flue gas channel. The sample intake is located close to the secondary superheaters temperatures and chloride gas-particle separation in such temperatures where alkali chlorides are in condensed phase and hydrogen chloride in gas phase. Between these temperatures is the area where alkali chloride vapours condense. This is also the area where condensation losses occur.

4.2. Sampling probe

The operation of the pre-separator is based on high circulating flow velocity which prevents fouling; only a small part of circulating flow is lead to the analyzer. The operation of coarse particle pre-separator is also based on high flow velocity. The circulating flow is created by an ejector and the flow is dimensioned to keep the sampling probe and filter clean. The sampling probe (figure 4-3) is designed to take gas phase chloride trough ceramic filter and total chloride sample through a virtual impactor which removes coarse particles out of sample. In the figure 4-4, the sampling device without heat insulation is presented. The sampling probe is located through the T-corner, in the lower side of the figure.

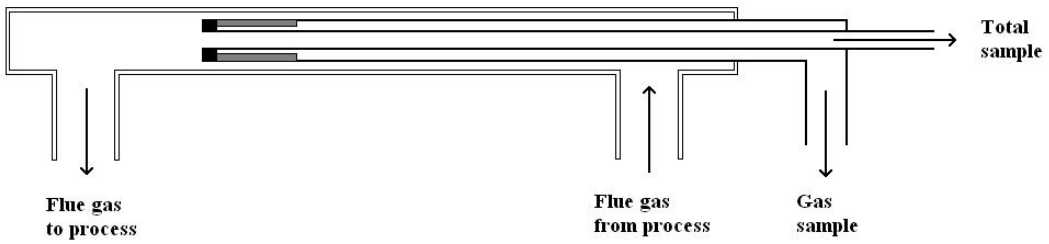

Figure 4-3: *Sampling probe*

Figure 4-4: *Sampling device without the heat insulation*

4.2.1. Coarse particle pre-separator

The U-turn particle pre-separator is shown in the figure 4-5. It is designed to decrease water insoluble species in analyzed sample, to prevent fouling in fast cooling region and to decrease disturbing particle components. The pre-separator operates as a virtual impactor; coarse particles can't follow streamlines to sampling by their inertia. With 800 l/min volumetric floe, the flow velocity in the tube before virtual impactor is around 20 m/s and about 40 m/s in the slot. The sample flow is 10 l/min which means the velocity of 6 m/s in the sampling inlet.

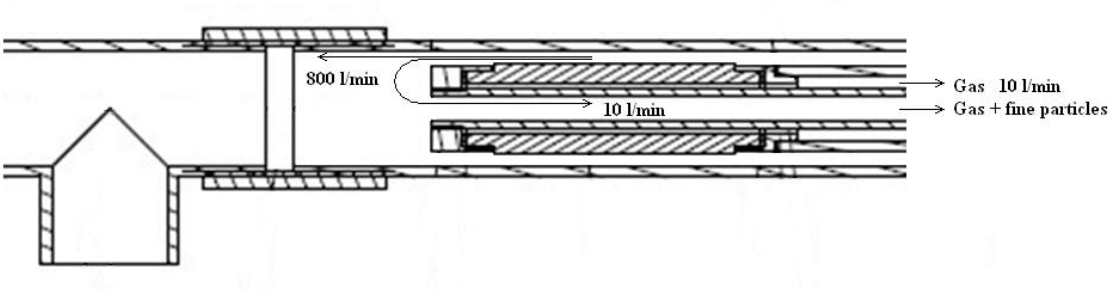

Figure 4-5: *U-turn coarse particle pre-separator*

4.2.2. High temperature filtering

The filter is used to separate gas phase chloride (HCl) from condensed chloride. The ceramic surface filter used is made of aluminum oxide and silicon carbide membrane. The filter is designed to operate at high temperatures, maximum temperature resistance is up to 1000 °C. In this use the operation temperature is lower than alkali chlorides condensation temperature 500 °C. Filter is located in the head of the sampling probe, where the flow velocity is 40 m/s, to prevent fouling by high flow velocity in slot (figure 4-5).

5. MEASUREMENTS

5.1. Virtual impactor measurements

The pre-separator was tested in laboratory. The aim of these tests were to determine the cut point of virtual impactor, the effect of flow velocity and the effect of sampling probes head shape. The virtual impactor principle was scaled on smaller size for these cut point measurements. These tests were also carried out at room temperature. In section 5.1.3 the measured values are compared with the theoretical calculations and the cut points in the real conditions are calculated based on measurements.

5.1.1. Measurement set up

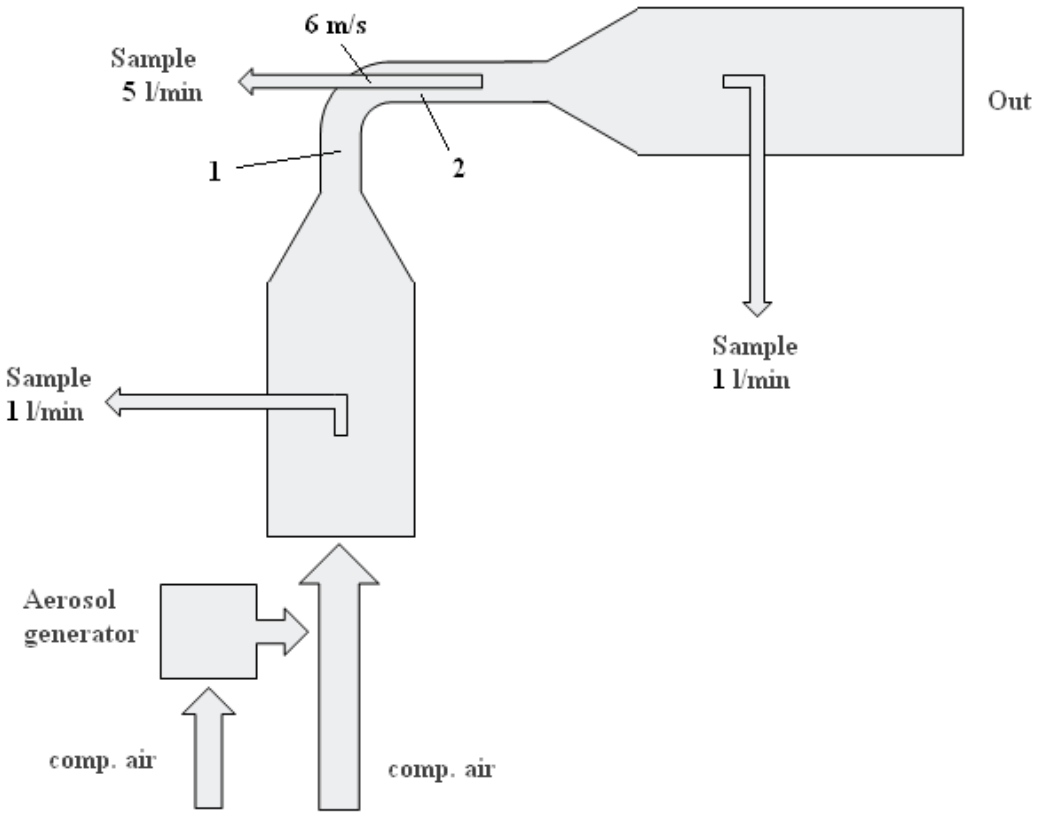

Figure 5-1: *The cut point measurements set up*

The laboratory pre-separator was dimensioned for 280 l/min flow and 5 l/min sample flow by keeping the flow velocities same as in full scale conditions. The inner diameter of the bend was 24 mm and the diameter of sampling probe was 17 mm. Other flow velocities were also tested in range of the isokinetic sampling. The flow velocities were varying around 20 m/s in location 1 and 40 m/s in the slot between bend and sampling probe (location 2 in the figure 5-1). Samples were taken at three locations; from the pre-separator sampling line and before and after the bend. Before and after virtual impactor the flow velocities were slowed down by widening sampling tube, slower velocity makes isokinetic sampling possible. At the beginning of the sampling system were located barriers to mix sample uniformly.

The particle size distribution was measured by TSI 3321 aerodynamic particle sizer (APS) which provides high-resolution, real-time aerodynamic measurements of particles from 0,5 to 20 μm. APS determines the aerodynamic size of particles by acceleration, with larger particles accelerating more slowly due to increased inertia. As particles exit the acceleration orifice they cross through overlapping laser beams in the detection area. Light scattered from each particle is converted to the electrical pulses by an avalanche photodetector. The APS spectrometer uses douple-crest optical system operating at 4-nanosecond resolution (TSI 2004).

The operation and stability of particle generators were tested with the Dekati electrical low pressure impactor (ELPI). ELPI is a real-time particle size analyzer designed for the range of 0,007–10 μm. ELPI consists of an aerosol charger and a cascade impactor. The electrical detection is made by multichannel electrometer. The flow velocities were set based on the pressure difference on a laminar flow element (Keskinen et al. 1992, Marjamäki et al. 2000).

For the first test series the particles were generated with the Palas RBG 1000 brush generator with test dust and fly ash. The generator setups were about 20 mm/h feed rates, 4 bar pressure and 1000 rpm. The flow trough RBG 1000 was 40 l/min and the total flow was varied around 280 l/min. Because of small particle size of the test dust and unstable distribution of fly ash the flow velocity. The next tests were carried out with sodium chloride particles generated by nebulizer.

During these measurements the flow varied from 70 to 330 l/min which means 10,2 and 48,3 m/s velocities in the slot respectively. In the end of test period liquid DOS (dioctyl sebacate) particles were also tested. The scaled laboratory pre-separator is presented in the figure 5-2. The changeable head is in the right in the figure. The virtual impactor is designed the way that the head can be changed without turning the flow down. Tested heads, 6 mm, 8 mm, sharp, hat and low hat are presented respectively in the figure 5-3. The 6 mm head is dimensioned based on the full scale probe were the filter is located in the head of the probe.

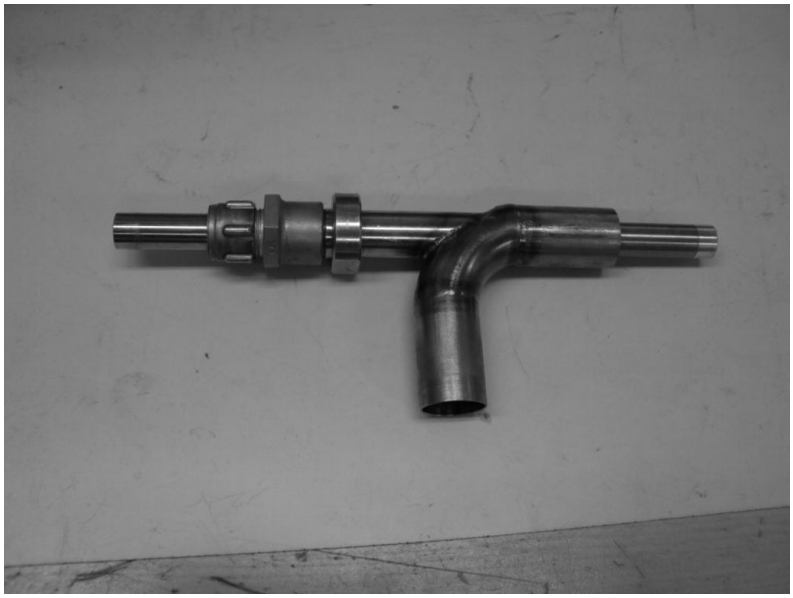

Figure 5-2: *Tested virtual impactor*

Figure 5-3: *Sampling probes heads*

5.1.2. Measurement results

In the figure 5-4 the particle size distributions from different locations generated by the brush generator are shown. The x-axis represents the aerodynamic diameter of the particle. The lower particle concentration of the sample is clearly seen in the figure at diameters between 1 and 10 μm. The fly ash contained also particles over 10 μm but those were lost in sampling system before the measurements. In the figure 5-5 the collection efficiencies calculated from the figure 5-4 data are shown. The virtual impactor cut point is around 2,5 μm with room temperature and 40 m/s in the slot. The calculated cut point of bend in sampling probe is about 10 μm which can be seen in the outlet collection efficiency.

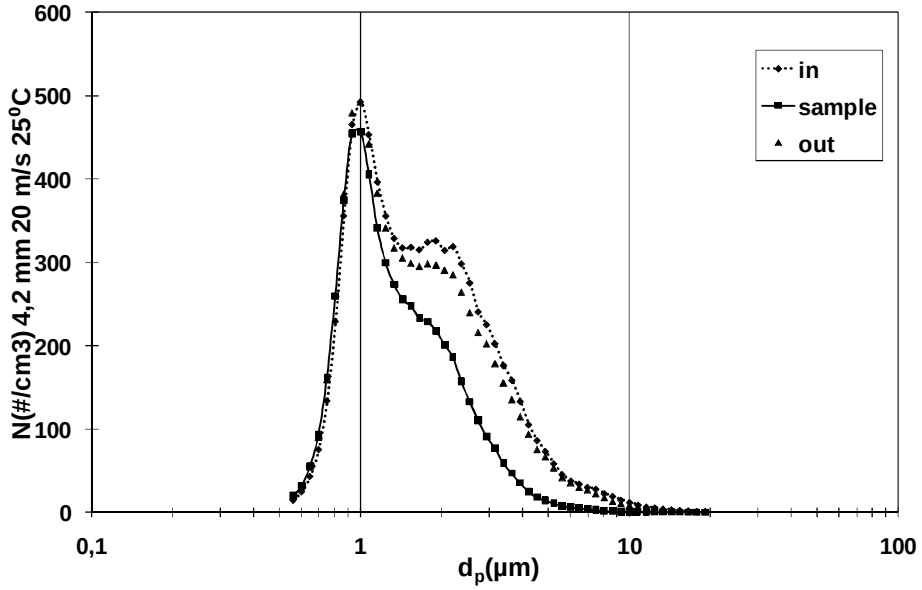

Figure 5-4: *Brush generator particle size distributions*

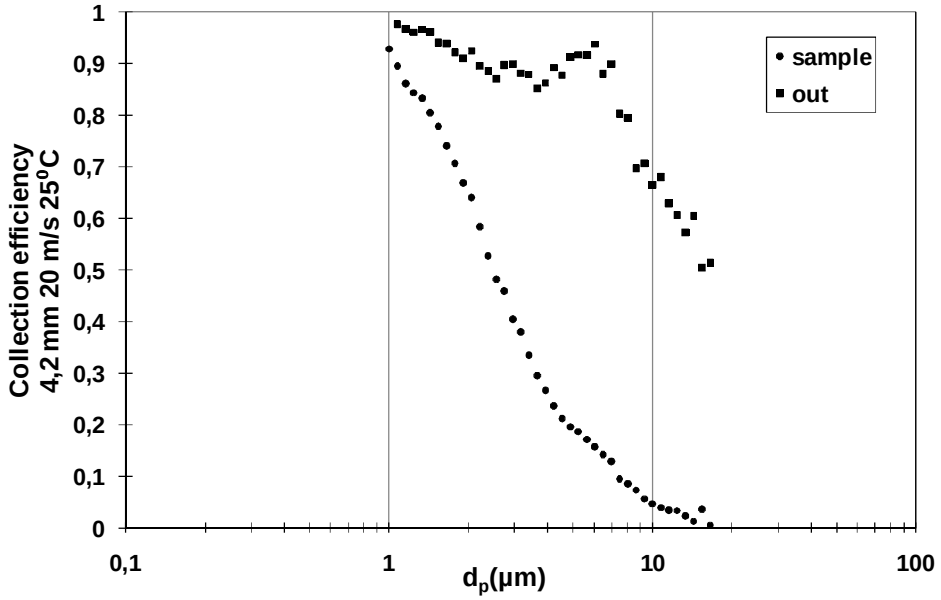

Figure 5-5: *Collection efficiencies of the virtual impactor and the bend*

The aerosol particle size distribution, generated by brush generator from fly ash, was unstable because of very rough composition of fly ash and generator properties. In the figure 5-6 the results of five measurement series at same conditions are presented. In some cases the collection efficiencies over 1 was detected. In this case that might be caused by the unstable particle distribution. The figure 5-7 presents the calculated standard error and average from figure 5-6 data. Despite unstable particle generation the measured series are close each other and the standard error is small.

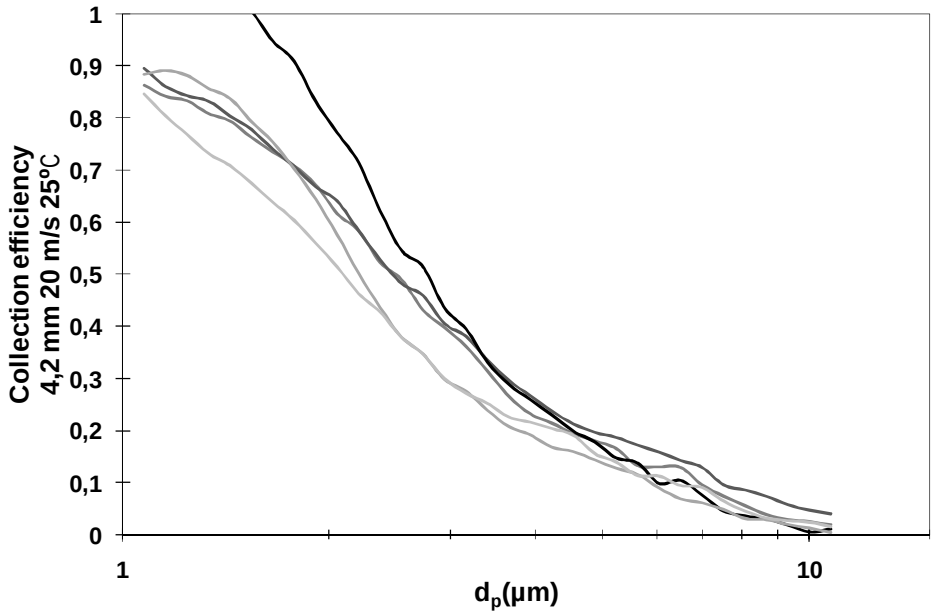

Figure 5-6: *Five measurement series at same condition*

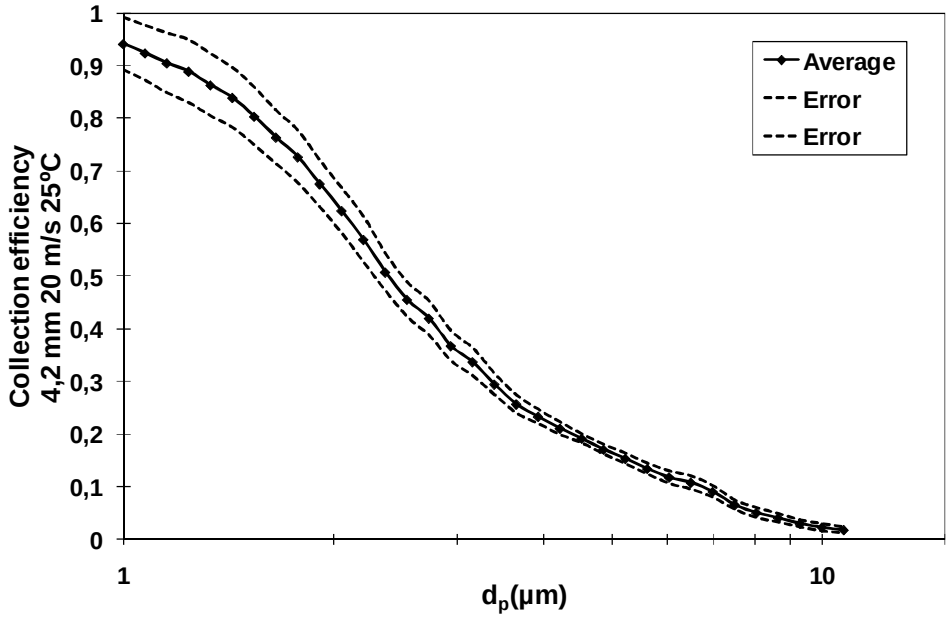

Figure 5-7: *Standard error from the figure 5-7 measurement series*

In the figure 5-8 the fixed collection efficiencies measured at same condition with low hat- head are shown. Different sampling probe heads were also tested with brush generator and 40 m/s flow, the fixed collection efficiencies are illustrated in figure 5-9. All collection efficiencies go one on the other when efficiencies are scaled to one. Differences in the raw data are possibly caused by unstable particle generation. There were not great differences with the structures of the head and no significant difference on the collection efficiency between the head was detected.

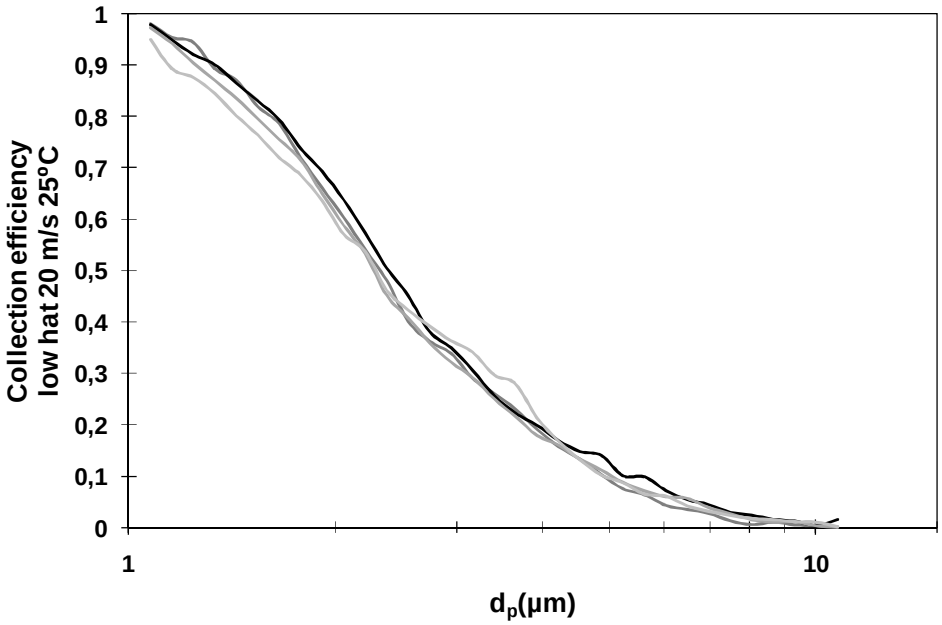

Figure 5-8: *Fixed collection efficiencies of four measured series at same condition*

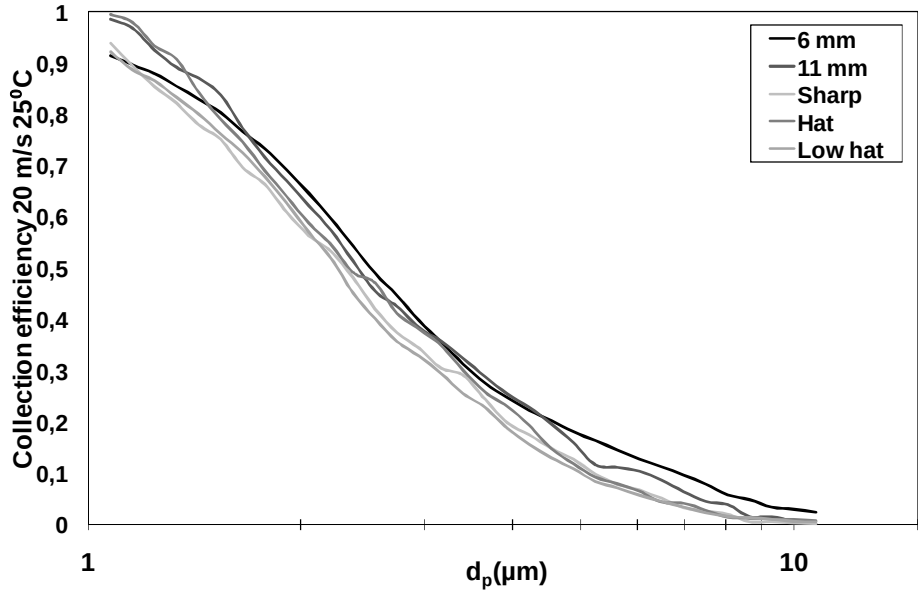

Figure 5-9: *Fixed collection efficiencies with different sampling probe heads*

In the figure 5-10 it is presented the results of the flow velocity effect measurements carried out with sodium chloride particles at room temperature. As was suspected, the cut point decreases when flow velocity increases. With higher velocities (40 and 50 m/s) the collection efficiency for fine particles is also decreased but the collection efficiency of larger particles is not changed significantly. The cut points of pre-separator are about 2,6 µm with 40 m/s in the slot and 3,25 µm with 20 m/s at laboratory conditions.

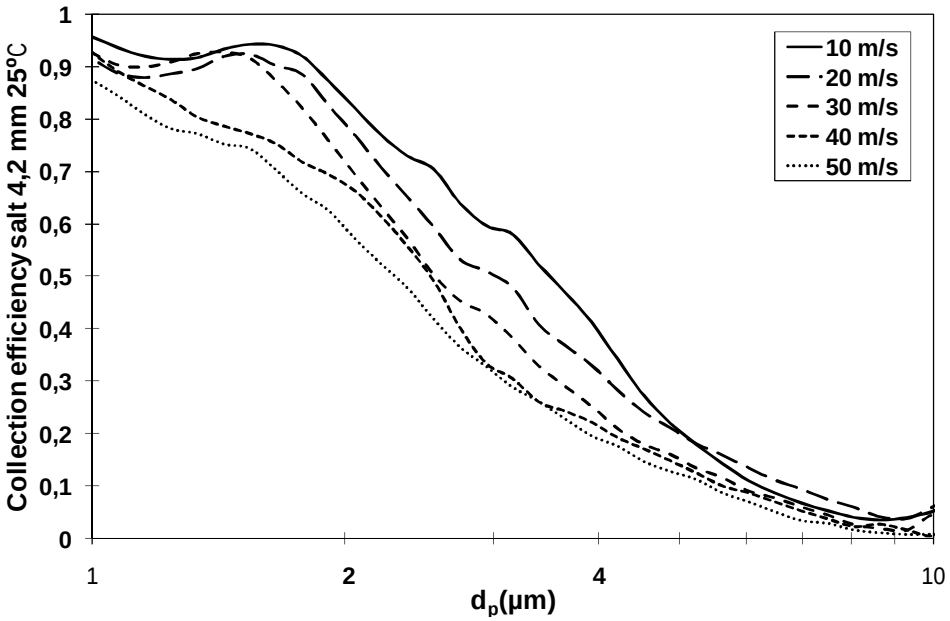

Figure 5-10: *Effect of the flow velocity on collection efficiency*

During these measurements no risk of blocking or serious fouling was detected but the missing coarse particles and condensable vapours affect fouling properties in field conditions. With liquid particles the pre-separator was fully coated by DOS. This indicates that part of the aerosol particles are collected on the sampling devices walls. When solid particles collide and stuck on the wall they probably form larger lumps or layers which breakaway as one. Inlet tube and outlet tube were fully coated by the fine dust and particles. Larger than 10 µm particles, were effectively lost in the sampling line.

5.1.3. Stokes numbers

In the figure 5-11 the Stokes numbers calculated by equation 3-5 from measured collection efficiencies with different Reynolds numbers in the slot are shown. The cut point diameter and the square root of the cut point Stokes numbers as a function of Reynolds numbers are presented in the figure 5-12. The dot line represents the Stokes number and black line is the cut point diameter. The change of the Stokes number indicates that the turbulence and the flow properties have a strong influence on the virtual impactor operation and the collection efficiency. In the field conditions, the Reynolds numbers are about 8 000 with 40 m/s flow because of much higher temperature. Strongly turbulent flow probably also makes the collection efficiency curve less steep and decreases the effect of flow velocity on cut point.

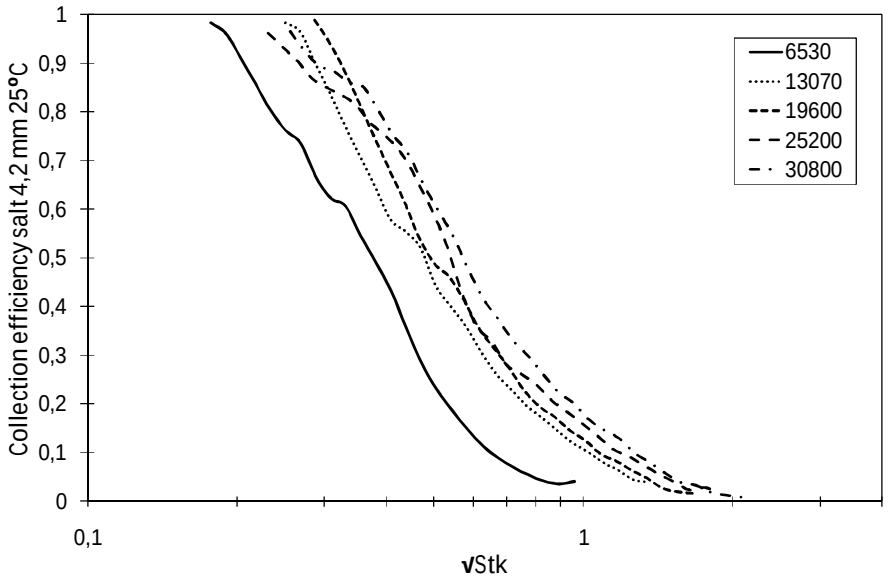

Figure 5-11: *Collection efficiencies at different Stokes and Reynolds numbers*

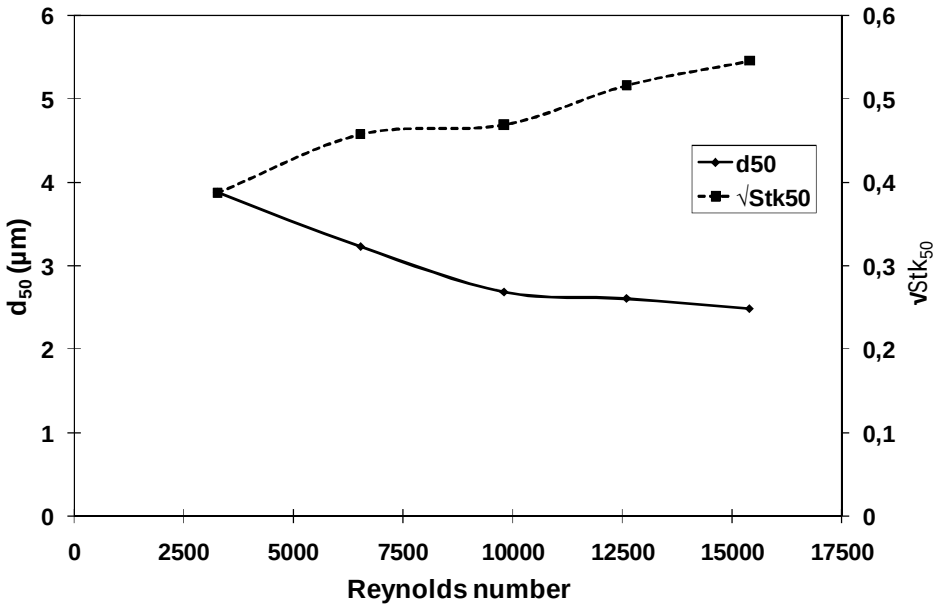

Figure 5-12: *The effect of Reynolds number on d_{50} (left axis) and √Stk_{50} (right axis) in laboratory conditions*

$$\sqrt{Stk_{50}} = 1{,}2524 * 10^{-5} * Re + 0{,}34613 \tag{5-1}$$

$$Re = \frac{U}{\mu}(D_o - D_i) \tag{5-2}$$

$$d_{50} = \sqrt{\frac{18\eta D}{\rho_p U C_c}} * \left(1{,}2524 * 10^{-5} * \frac{U}{\mu}(D_o - D_i) + 0{,}34613\right) \quad (5\text{-}3)$$

In the table 1 the measured and calculated cut points with velocities in the slot, Reynolds numbers and square root of Stokes numbers are presented. The Calc. d_{50} values are calculated by equation 5-3 where the jet diameter is 3 mm, D_o is 17 mm and D_i is 12 mm in laboratory. At field conditions the Reynolds numbers are around 3000–8000 and the equation 5-1 is determined from the lowest measured Reynolds numbers (3265, 6535 and 9800). The collection efficiency curve is also clearly different at higher Reynolds numbers. Measured and calculated cut points are close to each other at small Reynolds numbers because the equations 5-1 and 5-3 are determined at small Reynolds numbers.

Table 1: *Measured and calculated d_{50} values*

U (m/s)	Re_{tube}	Re_{slot}	Meas. d_{50} (µm)	√Stk_{50}	Calc d50 (µm)
10,2	5570	3265	3,88	0,3870	3,92
20,5	11150	6535	3,23	0,4576	3,06
30,7	16720	9800	2,69	0,4688	2,72
39,5	21490	12600	2,61	0,5162	2,53
48,3	26270	15400	2,49	0,5453	2,42

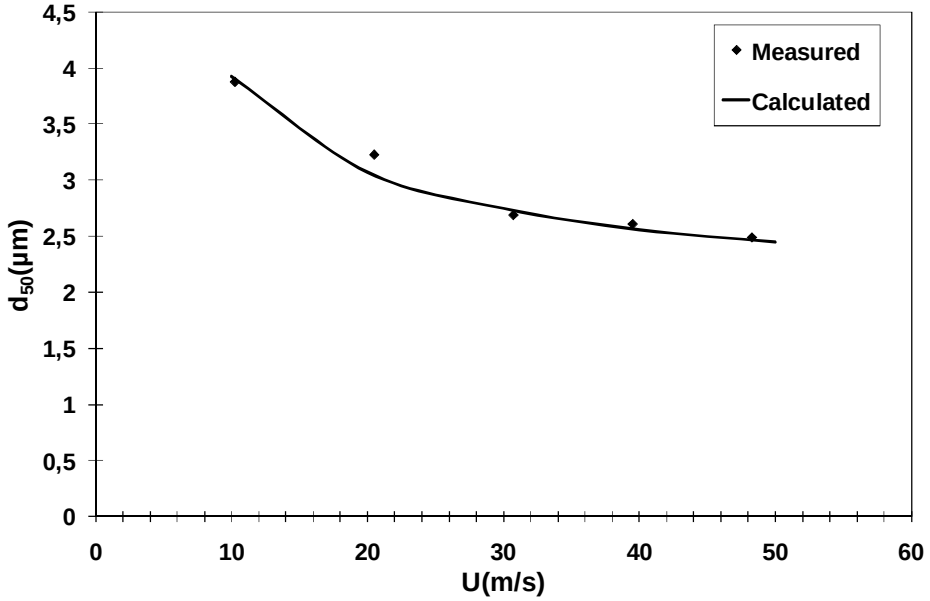

Figure 5-13: *The effect of the flow velocity to the cut point diameter at laboratory conditions*

5.1.4. Collection efficiencies in field conditions

The Reynolds numbers in the slot are at same level as in the tube and in field conditions. The flow in the slot is approaching laminar region when velocity is lower than 20 m/s. The collection efficiencies in field conditions in figure 5-14 are defined by approximating Stokes numbers with correct velocities and calculating Stokes numbers back to aerodynamic diameters by equation 5-1. In field the tube diameter is 4,35 mm, temperature 750 K and dynamic viscosity $3{,}48*10^{-5}$ kg/m/s. In table 2 the calculated cut points with Reynolds numbers and square roots of Stokes numbers are presented. The difference in the cut points compared to the laboratory conditions is mainly caused by the change of dimensions.

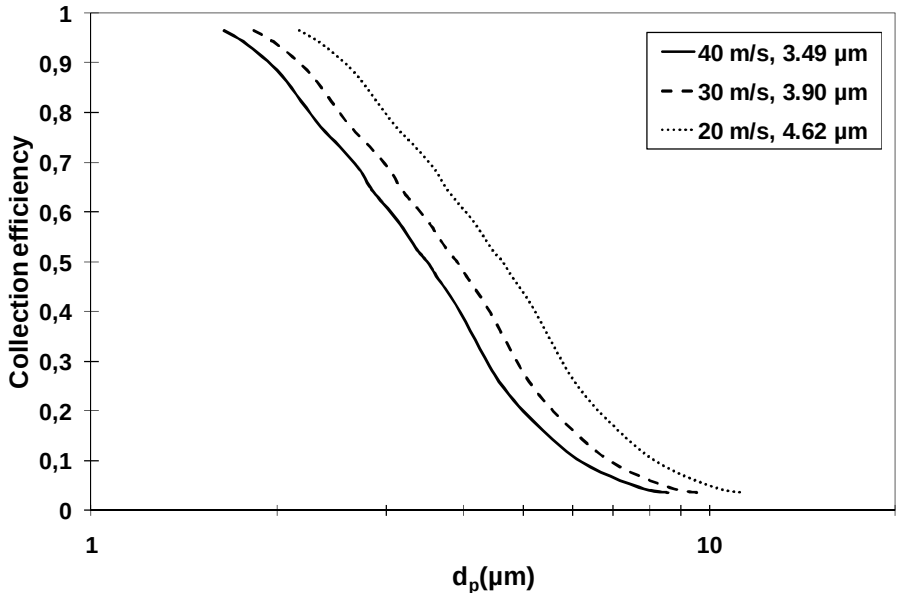

Figure 5-14: *Calculated collection efficiencies for the real sampling device and the temperature of 750 K*

$$d_p = \sqrt{\frac{18\eta D * Stk}{\rho_p C_c U}} \tag{5-4}$$

Table 2: *Calculated d_{50} in the field conditions at 750 K (Stk a function of Re)*

U_{slot} (m/s)	Re_{tube}	Re_{slot}	√Stk_{50}	d_{50} (µm)
20,0	4020	2350	0,376	4,62
29,9	5990	3525	0,390	3,90
39,9	8030	4700	0,405	3,49

In the figure 5-15 the calculated cut points at 1000 K temperature are shown. The cut points (table 3) are at same level as at 750 K because the temperature has reverse affect on Stokes numbers and viscosity. With the high temperatures the Reynolds numbers are relatively low and the flow properties might be different compared to the turbulent flow. When the temperature decreases the Stokes and Reynolds numbers also decreases.

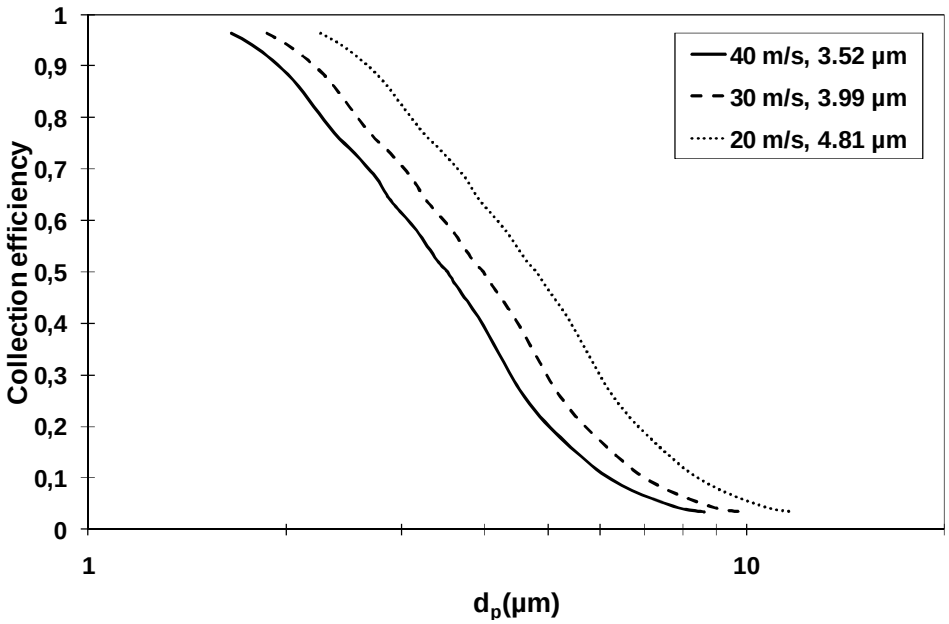

Figure 5-15: *The calculated collection efficiencies at 1000K temperature*

Table 3: *Calculated d50 in 1000 K*

U_{slot} (m/s)	Re_{tube}	Re_{slot}	$\sqrt{Stk_{50}}$	D_{50} (µm)
20,3	2550	1500	0,365	4,81
30,5	3850	2250	0,374	3,99
40,6	5100	3000	0,384	3,52

In the figure 5-16 the calculated temperature dependency of the cut point diameters in the field condition and size are shown. The change of the Stokes number decreases the effect of temperature and the flow velocity on the cut point. The theoretical effect of Reynolds number on the cut point diameter is presented in figure 5-17. In the figure 5-18 the calculated effect of flow velocity on d_{50} at temperatures 750 and 1000 K are presented.

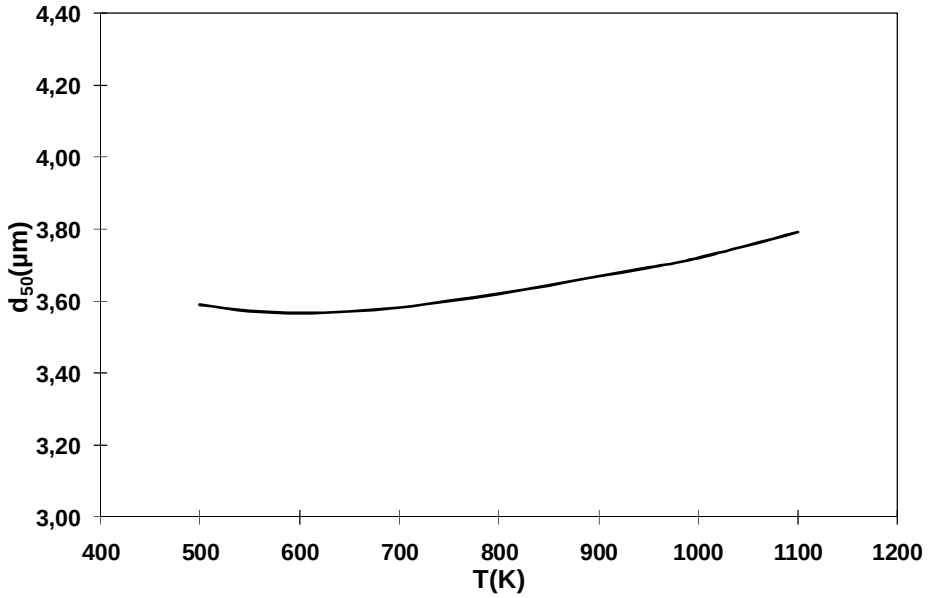

Figure 5-16: *The effect of temperature on the D_{50} in field conditions at 40 m/s flow velocity*

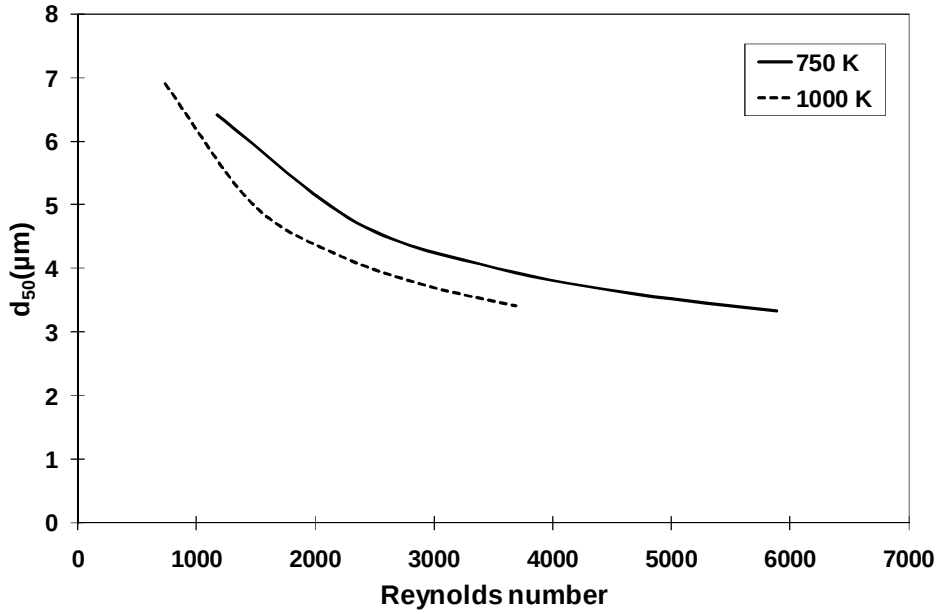

Figure 5-17: *The effect of Reynolds number on the cut point diameter in the field conditions*

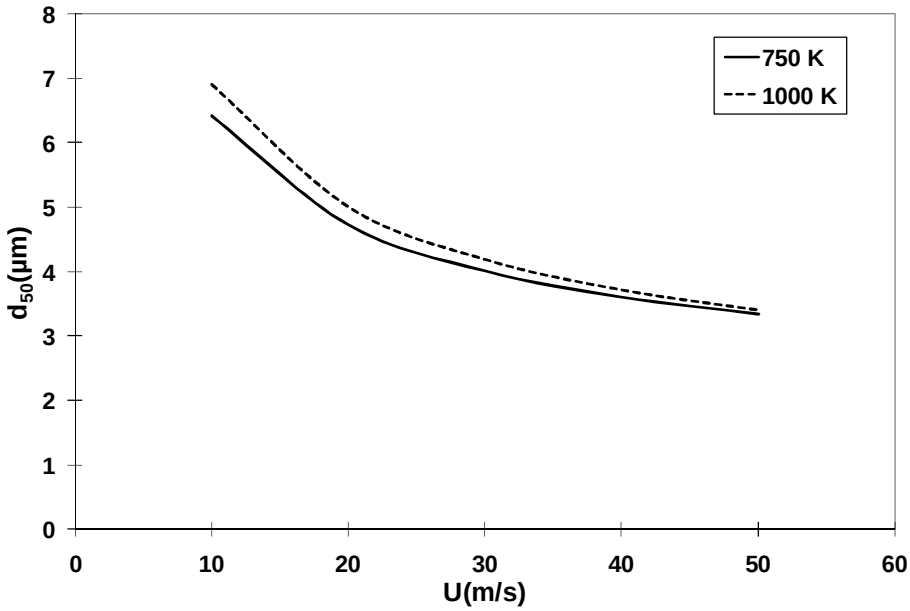

Figure 5-18: *The effect of flow velocity on the cut point diameter in the field conditions*

5.2. Pori field measurements

The circulating axial virtual impactor was first time tested in full scale during the larger measurement campaign in Pori Prosessivoima CFB boiler (figure 5-19). In the Pori campaign the RBDA measurement set-up was used to measure total Cl and K concentrations in the flue gas. The gas phase sample through the filter was not taken. The previously tested sampling probes were used in this test campaign as a reference method. Other references are from VTT fine particle measurements with the DLPI (Dekati low pressure impactor) and ELPI, fly ash analysis, FTIR and theoretical values.

Porin Prosessivoima
Pori
Finland

Steam	177 MW_{th} 67 kg/s 84 bar 522 °C
Fuels	Wood fuel, peat, recycled fuel, coal
Start-up	2008

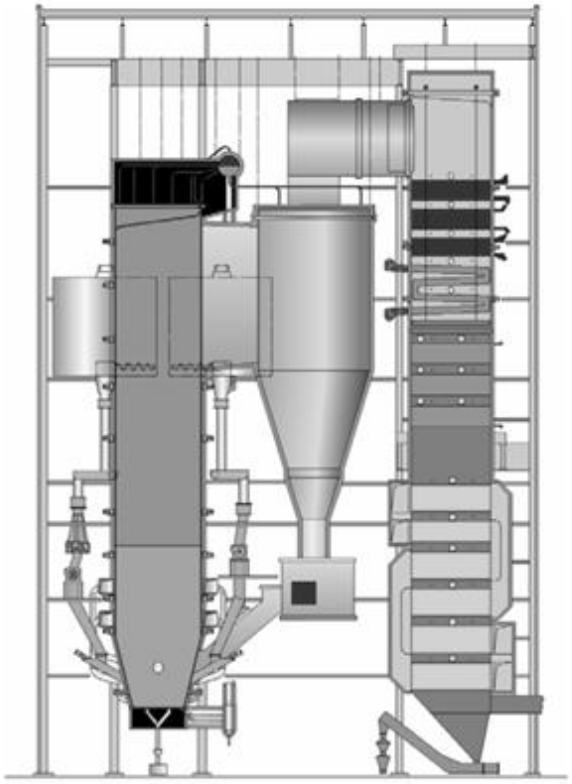

5-19: *Pori CFB boiler*

5.2.1. Results

The chloride measurement results are at same level as the reference measurements but the theoretical Cl total balance (figure 5-20) is much higher. The theoretical chloride level is calculated based on the fuel analysis and 0,08% Cl on the fuel. There might be great differences in the fuel quality especially for the recycled fuel. The measured levels corresponds to about 0,05% chloride on the fuel mix. In the figure 5-20 the potassium measurement results are shown. The *K in KCl Total (K/Na WS relat)* is calculated from the chloride in the particles based on the RBDA total chloride and the FTIR HCl (gas phase) chloride.

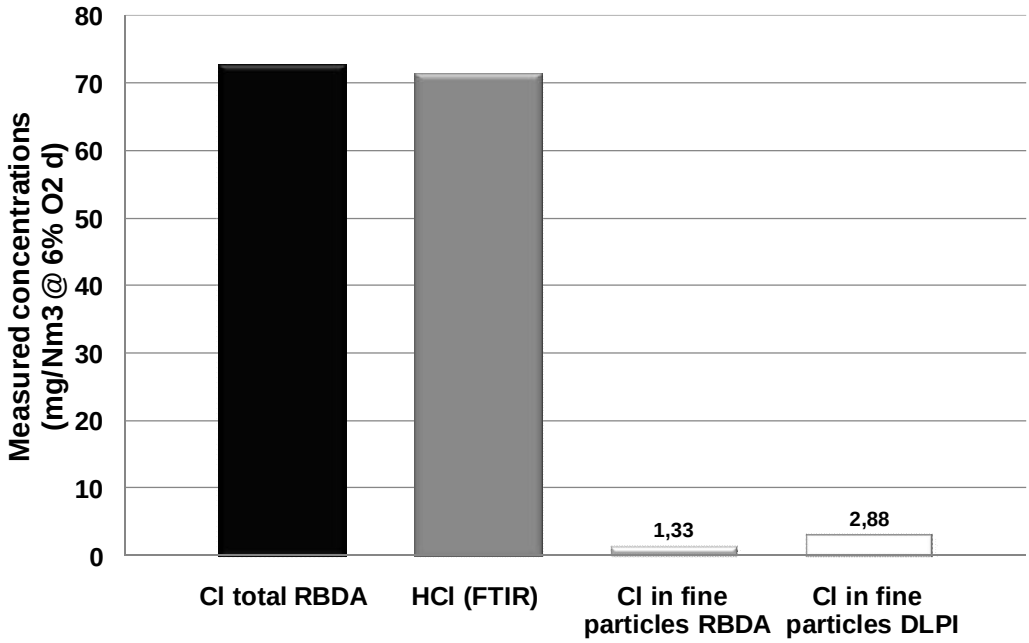

5-20: *Chloride levels from the RBDA and the reference measurements*

Sampling was, as expected, the biggest challenge in the measurement system. The sampling device had some problems with fouling (figure 5-21) and to up keep the circulating flow constant with the ejector. In the fast cooling regions the fouling has also caused losses especially for the alkalis due to the condensation and diffusion. The chlorine losses are clearly lower, since the main part of chloride exists in the form of HCl gas. The condensation losses can be reduced for example by bringing the KCl to the analyzer as vapour or by the dilution and controlled particle formation.

5-21: *Fouling on the head of the sampling probe*

5.3. KyVo field measurements

The aim of the Kymin Voima (figure 5-22) tests was to verify the sampling systems availability on long time on-line sampling and to test and develop the bubbling system. The gas sampling through the filter was also tested in the first time at KyVo. These tests were accomplished without the analyzer; instead the water samples were analyzed in the laboratory. The boiler load and chloride levels were low during these tests.

Kymin Voima,
Kuusankoski,
Finland

Steam	269 MW_{th} 107 kg/s 114 bar 541 °C
Fuels	Bark, forestresidue, sludge, peat, gas, oil
Start-up	2002

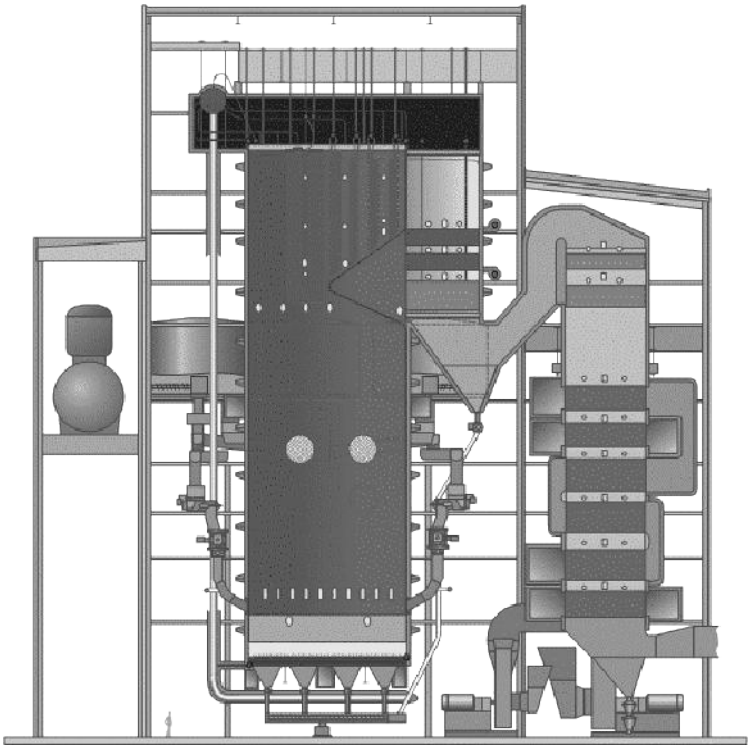

5-22: *KyVo BFB boiler*

5.3.1. Results

The measured chloride levels (figure 5-23) are a bit low, 10 mg/Nm^3 in the flue gas means under 0,01% chloride in the fuel. The low boiler load might have also affected the results. Because of the low chloride and higher sulphur levels the amount of alkali chloride should be low and the most of the chloride in the form of HCl gas. The measured gas phase chloride (HCl) levels are low compared to total chloride levels. During these tests the gas samples chloride levels were couple time greater than the total sample.

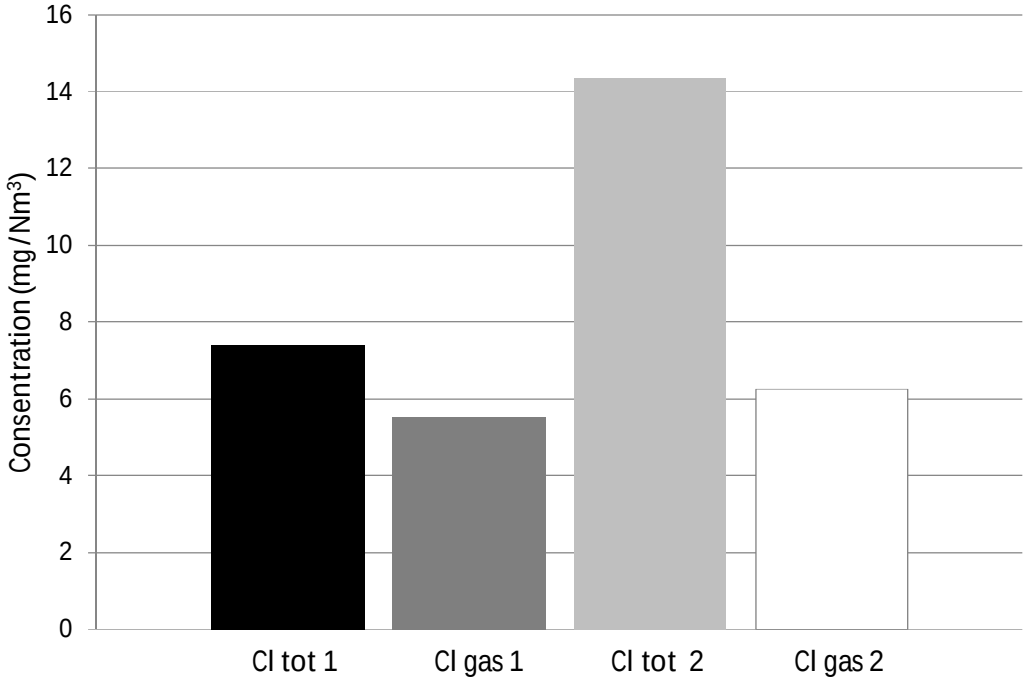

5-23: *Two test points from the sampling device tests at KyVo*

There were some problems with the fouling at circulating parts of the sampling device (figure 5-24) and with the leakages in the filters brackets. However, the sampling device was tested continuously for three weeks. After the three weeks test there was noticeable erosion in the ejector, which can be a problem in continuous use. No fouling at the sample lines after the pre-separator and the filter were detected. The sample can be collected with the bubbling container.

5-24: *Fouling from the sampling device before the pre-separator*

6. CONCLUSIONS

The combustion of the challenging bio and waste fuels containing high amounts of chloride and alkalis has become more important in the recent years. This development with the interest to use higher steam parameters has increased the importance to recognize the superheater high temperature corrosion. The aim of this thesis was to test and develop furnace alkali chloride sampling device including coarse particle pre-separator operating as a virtual impactor. The pre-separator operation and collection efficiency was tested in laboratory and the suitability to field conditions was tested in several full scale boilers.

The tested virtual impactor is able to cut coarse particles from the sample and it can be used to prevent the fouling. At the field conditions the cut point of the pre-separator is around 4 μm. The fine mode of the particle size distribution from the biomass combustion is under 1 μm. The better separation of this fine mode from total sample is very difficult. The structure must be very simple because of the heat expansion and fouling conditions limits the use of smaller dimensions in the coarse particle pre-separator. The cut point can be decreased by increasing the flow velocity. The structure of the sampling probes head does not significantly affect the cut point diameter or the collection efficiency.

The cut point of the virtual impactor can be estimated by the Stokes equation, but the effect of turbulence on Stokes number must be considered. The Stokes number describes the ratio of the particles mechanical mobility to dimension of the obstacle and is dependent of the fluid and flow properties. The flow properties can be taken into account by the Reynolds number. The turbulent flow can cause losses. If fine particles are collided on walls and separated as coarser particles some of measured species might be lost in the pre-separator.

Temperature does not significantly affect the cut point diameter at the temperature range from 500 to 1100 K. The cut point reaches the minimum at 600 K and grows slowly when the temperature is decreased or increased. When the flow velocity increases to over 20 m/s the effect of velocity on the cut point diameter decreases. In the laboratory conditions the effect of the flow velocity almost disappears when the velocity is greater than 30 m/s. These effects are caused by the opposed effect of the temperature (viscosity) and the flow velocity on the Reynolds number and the Stokes number.

The challenging boiler conditions and especially the high suspension atmosphere with the condensable vapours can cause problems for sampling device and/or sample handling system in the analyzer. Fouling can choke lines, cause pressure losses or even block the sampling device. Pressure losses can significantly affect on operation of the ejector and on the sample mass flow. The parts of sampling device after the pre-separator are protected from the fouling but some other parts of the sampling device can exposure to the fouling. When the circulating flow is made by an ejector the consumption of the pressurized air is a great source of expense. These expenses can be decreased by using smaller tubes and slower flow velocities.

The other problem to be solved is the sampling line loss. Between the sample intake (850 °C) and filter the sample needs to be cooled less than 500 °C. Between these temperatures the alkali chlorides condense and at same time the condensation on the sampling line or the cooler walls occurs. Also thermophoresis in the fast cooling regions and the diffusion causes losses especially for the fine particles. When the gas temperature decreases on the condensation region the alkali chlorides are also condensed on the larger particles which can’t follow the streamlines to the total sampling containing fine particles and gas. Losses can be decreased by keeping the potassium chloride in the vapour phase as long as possible. The nucleation after the dilution is one possibility to elude condensation losses.

REFERENCES

Abd-Elhady M., Rindt C., Wijers J., van Steenhoven A., Bramer E. and van der Meer Th.H., Minimum gas speed in heat exchangers to avoid particulate fouling, International Journal of Heat and Mass Transfer 47 3943-3955, 2004

Aho M., Vainikka P., Taipale R. and Yrjäs P., Effective new chemicals to prevent corrosion due to chlorine in power plant superheaters, Fuel 87, 647-654, 2007

Baron P. and Willeke K., Aerosol Measurement, principles, techniques, and applications, second edition, by John Wiley & Sons, Inc, 2005

Baxter L., Miles T., Miles T. Jr., Jenkins B., Milne T., Dayton D., Bryers R. and Oden L., The behavior of inorganic material in biomass-fired power boilers: field and laboratory experiences, Fuel Processing Technology 54, 47-78, 1998

Baxter L., Improved Recovery Boiler Performance Though Control of Combustion, Sulfur, and Alkali Chemistry, DOE/OIT/Forest Products, American Forest & Paper Association, Brgham Young University, 2008

Blomberg T., Which are the right test conditions for the simulation of high temperature alkali corrosion in biomass combustion?, Materials and Corrosion, Volume 57 Issue 2, 170-175, 2006

Brunner T., Obernberger I., Brouwers J. aand Preveden Z., Efficient and economic dust separation from flue gas by the rotational particle separator as an innovative technology for biomass combustion aand gasification plants, Proc. Of 10th European Bioenergy Conference, 8-11 June 1998

Christensen, Kurt A. and Livbjerg, Hans (1996) 'A Field Study of Submicron Particles from the Combustion of Straw', Aerosol Science and Technology, 25: 2, 185 — 199, First published on: 01 January 1996

Christensen K. A. and Livbjerg H., A Plug Flow Model for Chemical Reactions and Aerosol Nucleation and Growth in an Alkali-Containing Flue Gas, Aerosol Science and Technology 33:470-489, 2000

DEKATI Measurements Ltd, Continuous analysis of fly -ash particles in Kraft recovery-boiler flue gases, pointed at 25.10.2010 http://www.eibis.com/eibis/eibiswww/eibisdoc/4109en.htm#form, 2002

Enestam S., Fabritius M., Hulkkonen S. And Röppänen J., Control of ash operational problems in BFB combustion of biofuels and waste, Proceedings of ASME: 17th International (ASME) conference on Fluidized Bed Combustion, 2003

Hinds W, Aerosol Technology: properties, behavior, and measurement of airborne particles, 2nd edition, by John Wiley & Sons. Inc, 1999

Hulkkonen S., Fabritius M., and Enestam s., Fortum Engineering Ltd, Application of BFB technology for biomass fuels: Technical discussion and experiences from recent projects, Proceedings of ASME: 17th International (ASME) conference on Fluidized Bed Combustion, 2003

Jimenez S. and Ballester J., Formation of alkali sulphate aerosols in biomass combustion, Fuel, 86, 486-493, 2007

Jokiniemi J. and Sippula O., Modeling fine particle formation and alkali metal deposition in BFB combustion, Finnish-Swedish Flame day 2009

Jöller M., Brunner T. and Obernberger I., Modeling of aerosol formation during biomass combustion for various furnace and boiler types, Fuel Processing Technology 88 1136-1147, 2007

Kassman H., Broström M., Berg M. and Å L.-E., Measures to reduce chlorine in deposits: Application in a large-scale circulating fluidized bed boiler firing biomass, Fuel, 90, 1325-1334, 2011

Kavidass S., Anderson G. and Norton G. jr., Why Build a Circulating Fluidized Bed Boiler to Generate Steam and Electric Power, POWER-GEN Asia, BR-1708, 2000

Keskinen J., Pietarinen K. and Lehtimäki M., Electrical low pressure impactor, Journal of aerosol Scinece 22, 4, 1992

Koornneef J., Junginger M. and Faaij A., Development of fluidized bed combustion-An overview of trends, performance and cost, Progress in Energy and Combustion, 33 19-55, 2007

Livbjerg H., Aerosol Formation from Straw Combustion – Danish Experiences, Aerosols from Biomass Combustion, International Seminar at 27 June 2001 in Zurich (Switzerland), ISBN 3-908705-00-2 Copyright © Verenum (Switzerland) 2001

Makkonen P, Neural Network for Prediction of Superheater Fireside Corrosion in CFB Boilers, Circulating Fluidized Bed Technology VI, Proceedings of the 6th International

Conference on Fluidized Beds, Werther J. (Ed), DECHEMA, Wurzburg Germany 1999, ISBN 3-89746-003-3, pp. 965-970

Marjamäki M., Keskinen J., Chen D.-R. And Pui D,Performance evalution of the electrical low-pressure impactor (ELPI), Journal of Aerosol Science, 31, 2, 2000

Metso, Brochures, Bubling Fluidized Bed (BFB) technology HYPEX boilers, 2010a

Metso, Brochures, Circulating Fluidized Bed (CFB) technology CYMIC boilers, 2010b

Miettinen Westberg H., Byström M. and Leckner B., Distribution of potassium, Chlorine, and Sulfur between Solid and Vapor Phase during Combustion of Wood Chips and Coal, Energy & Fuels, 17, 18-28, 2003

Mills A. F., Basic Heat & Mass Transfer, second edition, by Prentice Hall, Inc, 1999

Partanen Jatta, Chemistry of HCl and Limestone in Fluidised Bed Combustion, REPORT 04-1, Academic Dissertation Laboratory of Inorganic Chemistry, Åbo Akademi, 2004

Peltola K., Hiltunen M., Blomqvist J.-P., Skrifvars B.-J., Kurkela J., Latva-Somppi J. and Kauppinen E., Fouling of the Cooling Surfaces in Biofuel-Fired Fluidized Bed Boilers, Proceedings of the 15th International Conference on Fluidized Bed Combustion, FBC99-0185, 1999

Richardson A., Eshbaugh J., Hofacre K. and Gardner P., Respirator filter efficiency testing against particulate and biologigal aerosols under moderate to high flow rates, Aberdeen proving ground, MD 21010-5424. 2006

Riedl R., Dahl J., Obernberger I. and Narodoslawsky M., Corrosion in fire tube boilers of biomass combustion plants, Proceedings of the China International Corrosion Control Conference ’99, paper Nr.90129, 1999

Rönkkömäki H., Pöykiö R., Nurmesniemi H., Popov K., Merisalu E., Tuomi T. And Välimäki I., Particle size distribution and dissolution properties of metals in cyclone fly ash, Int. J. Environ. Sci. Tech, 5 (4), 485-494, 2008

Salmenoja K, Field and Laboratory Studies on Chlorine-induced Superheater Corrosion in Boilers Fired with Biofuels, Åbo Akademi, Kemisk-tekniska fakulteten, Report 00-1, Academic Dissertation, 2000

Silvennoinen J., Rantee A. and Töyrylä P., CHP Production Based on Co-Combustion of Demanding Biomass Fuels in a Bubling Fluidized Bed Boiler, Presented at Power Gen Europe 2004 Conference, 2004

Sippula Olli, Fine Particle Formation and Emissions in Biomass Combustion, Report series in Aerosol Science, N:o 108, 2010

Skrifvars B.-J., Lauren T., Hupa M., Korbee R. And Ljung P., Ash behaviour in a pulverized wood fired boiler - a case study, Fuel 83, 1371-1379, 2004

Strand, M. , Bohgard, M. , Swietlicki, E. , Gharibi, A. and Sanati, M.(2004) 'Laboratory and Field Test of a Sampling Method for Characterization of Combustion Aerosols at High Temperatures', Aerosol Science and Technology, 38: 8, 757 — 765, First published on: 01 August 2004

TSI, Aerodynamic Particle Sizer Spectrometer model 3321, pointed at 28.12.2010, http://tsi.hosting.onvoy.com/documents/3321.pdf, 2004

Vainio E., Brink A., Vesala H., Tormonen K. And Hupa M., Extractive determination of the flue gas composition in a recovery boiler furnace, Joint Meeting of the Scandinavian-Nordic and French Sections of the Combustion Institute, Copenhagen, 2009

Valmari T., Lind T. M. And Kauppinen E., Field Study on Ash Behaviour during Circulating Fluidized-Bed Combustion of Biomass. 1. Ash Formation, Energy & Fuels, 13, 379-389, 1999

Von der Weiden S.-L., Drewnick F. and Borrmann S., Particle Loss Calculator – a new software tool for the assessment of the performance of aerosol inlet system, Atmospheric Measurement Techniques, 2, 479-494, 2009

Zeuthen J. H., Jensen P. A., Jensen J. P. and Livbjerg H., Aerosol formation during the Combustion of Straw with Addition of Sorbents, Energy & Fuels, 21, 699-709, 2007